A MEASUREMENT SYSTEM FOR TURBULENCE PROPERTIES IN A THREE-DIMENSIONAL FLOW USING A DATA LOGGER

by

Ronald Jett Harper

Thesis submitted to the Graduate Faculty of the

Virginia Polytechnic Institute and State University in

partial fulfillment of the requirements for the degree of

MASTER OF SCIENCE

IN

MECHANICAL ENGINEERING

APPROVED:

F. J. Pierce, Chairman

W. C. Thomas

H. P. Marshall

March 1985

Blacksburg, Virginia

A MEASUREMENT SYSTEM FOR TURBULENCE PROPERTIES IN A THREE-DIMENSIONAL FLOW USING A DATA LOGGER

by

Ronald Jett Harper

ABSTRACT

An analysis is presented for hot wire/film anemometer measurement of mean velocities and turbulent stresses in a three dimensional flow field with a predominant flow direction. The experimental data can be taken with an automated traverse under the control of a digital data acquisition system which has been modified for this particular application.

ACKNOWLEDGMENTS

I thank Professor F. J. Pierce for serving as the chairman of my advisory committee.

I also thank the other committee members, Professors W. C. Thomas and H. P. Marshall, for their service.

I am grateful to fellow students Dr. M. D. Harsh, Dr. J. D. Menna, I. K. Tree, and Dr. P. A. Treventi for their helpful assistance and advice.

Last, I thank who was the typist and illustrator of this thesis.

TABLE OF CONTENTS

Table of Contents (continued)

TABLE OF CONTENTS (continued)

LIST OF FIGURES

LIST OF FIGURES (continued)

LIST OF TABLES

NOMENCLATURE

A	anemometer performance equation intercept
A_T	trigonometric expression, MHK analysis
A'	anemometer performance equation intercept
A''	anemometer performance equation intercept
B	anemometer performance equation coefficient
B_T	trigonometric expression, MHK analysis
B'	anemometer performance equation coefficient
B''	anemometer performance equation coefficient
C_1	anemometer performance equation intercept
C_2	anemometer performance equation coefficient
C_T	trigonometric expression, MHK analysis
D_T	trigonometric expression, MHK analysis
d	diameter of sensor element
E	voltage, overall or mean value
E_T	trigonometric expression, MHK analysis
e	time variant voltage component
F_T	trigonometric expression, MHK analysis
h	Jorgenson cooling law pitch coefficient
I	current
k	Jorgenson cooling law yaw coefficient
ℓ	length of sensor element
n	exponent in anemometer performance equation
Nu	Nusselt number
P	pitch angle of sensor
Pr	Prandtl number

q	heat transferred from sensor element
R	resistance
Re	Reynolds number
S	linearized anemometer sensitivity coefficient
s	vector directed perpendicular to sensor support plane
T	temperature, or coordinate transformation sensor
t	coordinate transformation tensor quantity
U	velocity, overall or mean value
u	time variant velocity component
w	vector directed along sensor element
α	angle between sensor supports and normal to sensor element
γ	horizontal probe calibration yaw angle
δ	yaw angle of sensor
ε	velocity vs voltage equation sub-expression
θ	angle of horizontal component of streamline measured from tunnel axis
μ	viscosity
ϕ	pitch angle of probe
ψ	deviation of probe yaw angle from streamline vertical plane
ω	velocity pitch angle in vertical plane

Superscripts

$\sim$	sum of mean and time variant components
$-$	time average or mean

Subscripts

BN	binormal component
eff	effective

f	at fluid temprature
fp	full projection to flow
ℓ	linearized
n	normal direction
N	normal component
s	streamline direction
T	tangential component
w	at wire temperature
x	x direction
y	y direction
z	z direction
0	0° or reference conditions
180	180°
∞	freestream conditions

1. INTRODUCTION AND SCOPE

The objective of this research is to review the necessary analysis, and develop and check out a system for the measurement of mean velocities and turbulent stresses in a three-dimensional flow field dominated by a streamwise mean velocity. A hot wire/film anemometer is employed to provide the required data, and the data taking procedure is controlled by a digital data acquisition system.

The mean flow and turbulence properties follow from the analysis of McMahan, Hubbartt, and Kubendran (MHK) [1] using a single slant and a single horizontal sensor element.

Each probe is traversed vertically across the flow field. At each elevation, the probe is aligned in a vertical plane tangent to the local mean flow streamline, and then revolved about its axis to specified positions, at which measurements are made of mean and rms anemometer output voltages. These data are used in the MHK equations [1] to calculate mean velocities in the vertical plane tangent to the local streamline. Mean velocity components are obtained in both the horizontal and vertical directions in this plane. Additionally, the six turbulent stress tensor quantities in this local reference frame are obtained. A coordinate transformation is then performed to relate these mean velocities and turbulent stress terms to a laboratory x, y, z system.

The response equations for modeling the anemometer system depend heavily on the determination of calibration constants for the particular probes used. These constants relate anemometer output voltage to mean

velocity and angular orientation of the probe to the mean flow. These equations are also developed and presented.

An analysis is presented in Appendix A to relate yaw and pitch of the anemometer sensor element to yaw and pitch of the probe, to facilitate probe calibration.

A description of the tunnel and ancillary equipment is included, as well as a brief review of anemometer theory and the fundamental equations utilized.

Attention is also given to the automated traverse and digital data acquisition system [2] which have been modified specifically to suit the needs of this application.

The traverse moves the probe in vertical and axial rotation modes under the control of a Tandy Radio Shack TRS-80 Model III microcomputer [2,3,4,5]. The computer also sequences sampling of anemometer output signals, performs statistical analysis, and records data on a floppy disk for subsequent transmittal to an IBM mainframe for processing.

A program to reduce the data according to the MHK analysis has also been written and may be found in Appendix B.

2. MHK EQUATIONS FOR ANEMOMETER PEFORMANCE

McMahon, Hubbartt, and Kubendran [1] have presented an analysis of the relationship between anemometer outputs and mean velocity components and turbulent stresses in three-dimensional turbulent flows dominated by a streamwise mean velocity.

The analysis assumes a single slant and a single horizontal hot wire/film probe installed in a cross-flow configuration.

2.1 Derivation of the MHK Equations

The basic procedure for derivation of the equations for the mean velocities and turbulent stresses in a streamwise mean velocity dominated three-dimensional flow field is as follows:

1) The instantaneous velocity vector in the local s,y,n coordinate system is resolved into components in the normal, tangential, and binormal directions relative to the sensor and probe body. This is done to relate the different cooling effects that U_N, U_T, and U_{BN} have on the sensor according to the Jorgenson model for effective cooling velocity. The resolution is done in terms of the coordinates shown in Figure 2.1.

2) The velocity components are assumed to be made up of time average and turbulent fluctuation terms. These are used in the Jorgenson law. Assuming a linearized anemometer, the velocity expression is expanded into a series assuming U_s is the predominant local horizontal velocity component.

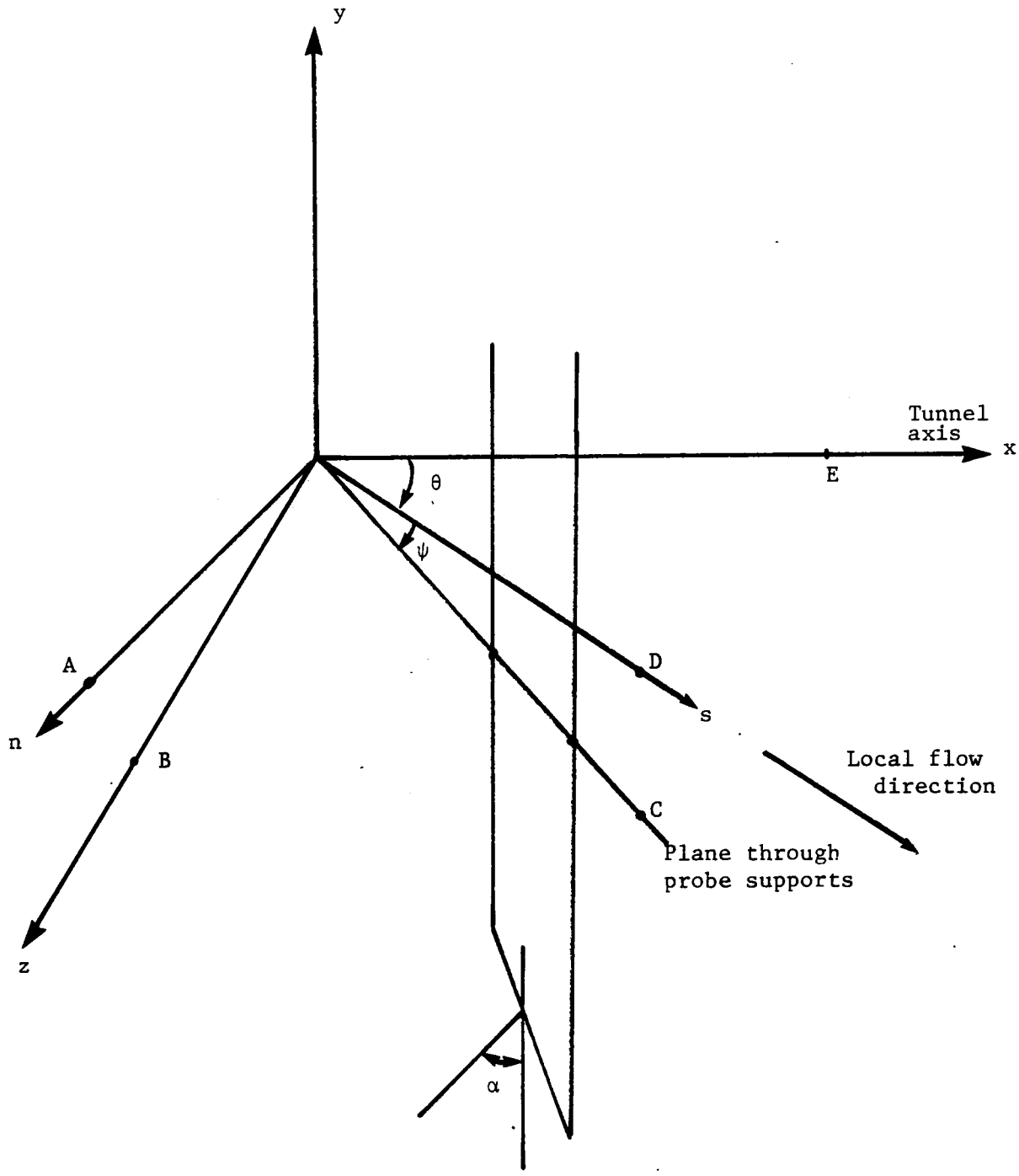

Points A, B, C, D, E are coplanar.
The short end of the probe is upstream of the long one at $\psi = \theta = 0$.

Figure 2.1 Tunnel Coordinate System

3) Various squaring and time averaging operations are performed to relate effective velocity to mean and rms voltages. The final result is two general response equations containing mean velocities, all turbulent stresses, and the mean and rms voltage quantities.

4) The general response equations are specialized at various angular positions of each probe (under the assumption of constant k and h in the Jorgenson cooling law) to yield equations which may be consecutively solved to relate voltage data to the mean velocities and turbulent stresses.

5) The velocities and stresses obtained are all relative to a local streamline coordinate system such that the transverse component of velocity is zero. A coordinate transformation is next performed to relate these s,y,n quantities to x,y,z laboratory coordinates.

2.2 Resolution of Velocity into Normal, Tangential and Binormal Components Relative to the Probe Sensor Element

2.2.1 Windtunnel Coordinate System Description

Figure 2.1 depicts the x, y, z (laboratory) and s, y, n (local streamline) coordinate systems and their relation to each other. Both systems are right handed and separately orthogonal.

The x coordinate is directed along the tunnel axis in the direction of flow. The y coordinate is vertical, upwards. The z coordinate is mutually orthogonal.

In general, the s,y,n coordinate system changes at each point in the flow. The s direction is found by rotating the probe body about the vertical y axis, through angle θ until an extremum in mean output voltage is found, which indicates that the sensor presents maximum length normal to the local streamline. The s coordinate is along the projection of the local flow velocity onto a horizontal plane. The y axis remains common to both the x,y,z and s,y,n systems. The n axis is mutually orthogonal or transverse to the local s and y axes. Note that there is no mean flow locally along the n axis, but only turbulent fluctuations. There can in general be a y (vertical) velocity component. The s and n velocity components are in a horizontal plane.

Note that the only rotational capability which exists for the probe body in the flow is about the y axis. The s and x axes define the angle θ, and further rotations of the probe about the y axis from the s direction define the angle ϕ.

It is through these two variable and measurable angles, θ and ϕ, that the normal, tangential, and binormal component directions are related to the laboratory coordinates.

The angle of the sensor to its supports (which is inherent in its manufacture) is defined as α in Figure 2.1. This angle also enters the analysis.

2.2.2 Decomposition of s,y,n Velocity Components to N,T,BN Components

An essential equation in this analysis is the Jorgenson law for effective velocity on an anemometer probe which is given by

$$U_{eff}^2 = U_N^2 + k^2 U_T^2 + h^2 U_{BN}^2 \tag{2.1}$$

where U_N, U_T, and U_{BN} are components of velocity in the normal, tangential, and binormal directions relative to the sensor, as depicted in Figs. 2.2 and 2.3 for horizontal and slant sensors, respectively.

To use this Jorgenson cooling law, it is necessary to determine the normal, tangential, and binormal velocity components in terms of the s,y, and n velocity components which are more readily measured in the laboratory. This is done by decomposing the s,y,n components of velocity individually into their N, T, BN components, and then adding together all components in each of these directions.

2.2.2.1 Decomposition of s Velocity Component

First, the s component of velocity will be decomposed into N,T,BN components. Figure 2.4 depicts the $\tilde{U}_s$ instantaneous component in the horizontal plane. It is decomposed into a BN component and a remainder. The remainder is shown in a vertical true length plane in Fig. 2.5 and is further decomposed into T and N components. Refer to Fig. 2.6 for an isometric view.

$$\tilde{U}_{s,BN} = \tilde{U}_s \sin \phi \tag{2.2}$$

$$\tilde{U}_{s,T} = \tilde{U}_s \cos \phi \cos \alpha \tag{2.3}$$

$$\tilde{U}_{s,N} = \tilde{U}_s \cos \phi \sin \alpha \tag{2.4}$$

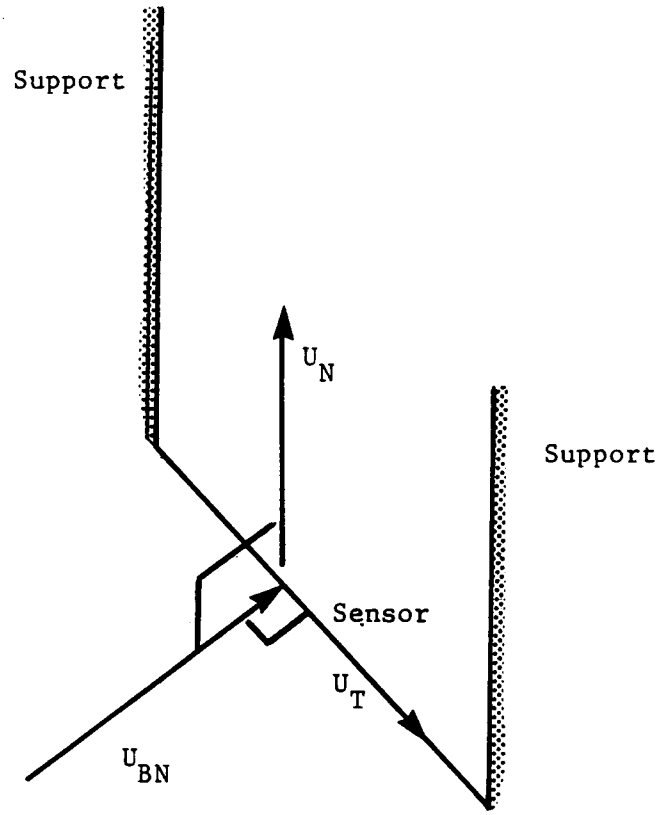

Figure 2.2 Illustration of Velocity Components on a Horizontal Anemometer Sensor

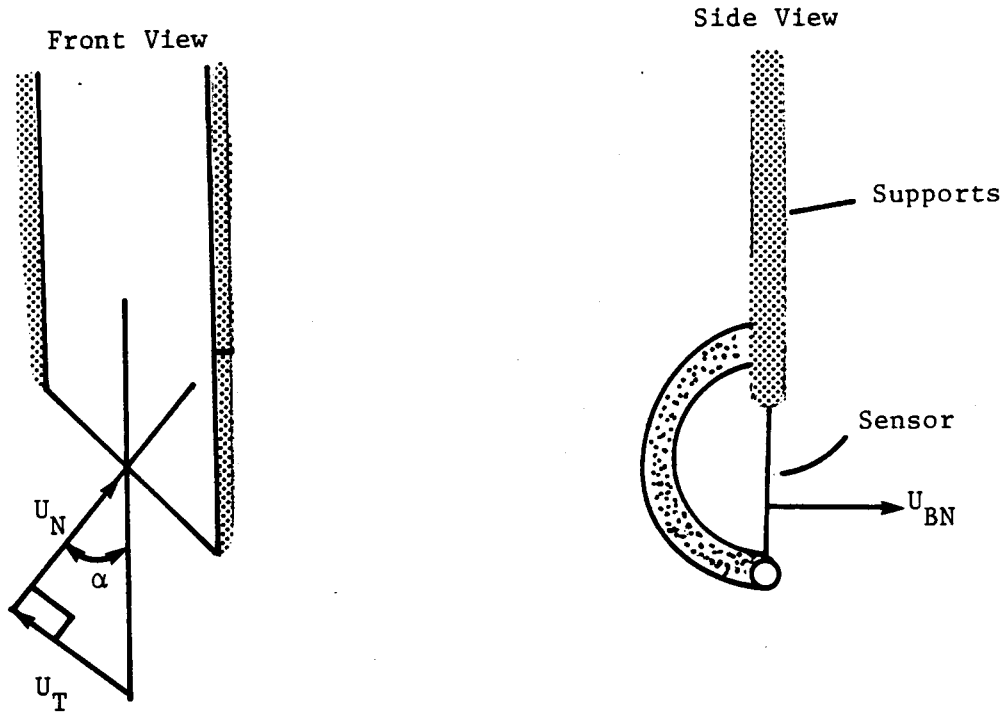

U_{BN} out of page

U_N, U_T are in the plane of the probe supports

Note the offset which is present on the longer probe support to avoid flow interference effects at $\psi = 180°$ position. (See also Fig. 3.6)

Fig. 2.3 Illustration of Velocity Components on a Slant Anemometer Sensor

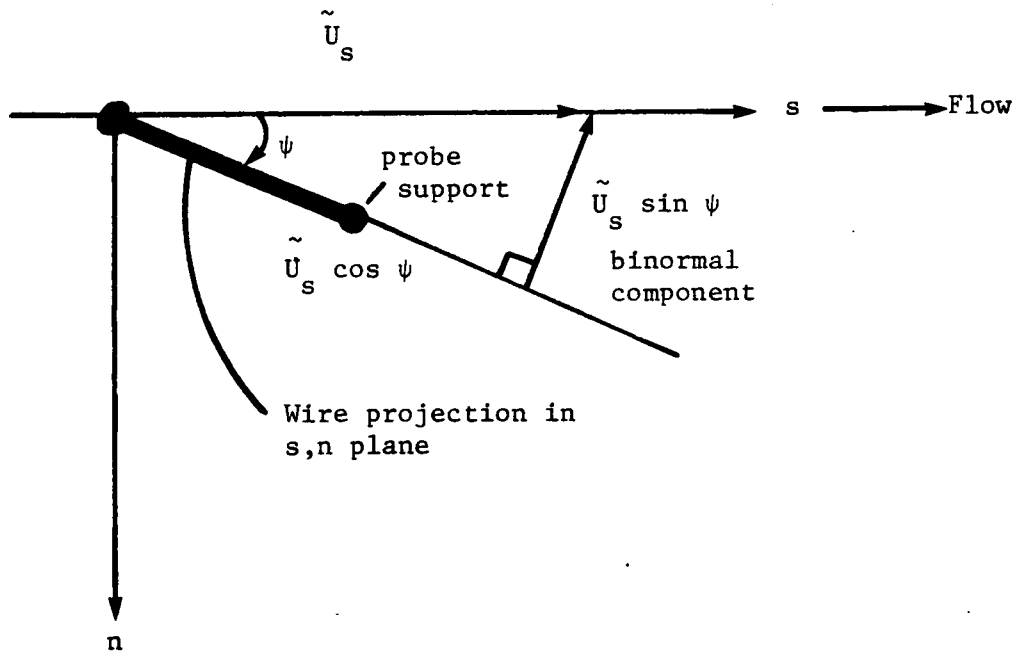

Figure 2.4 Decomposition of $\tilde{U}_s$ Velocity in s,n Horizontal Plane

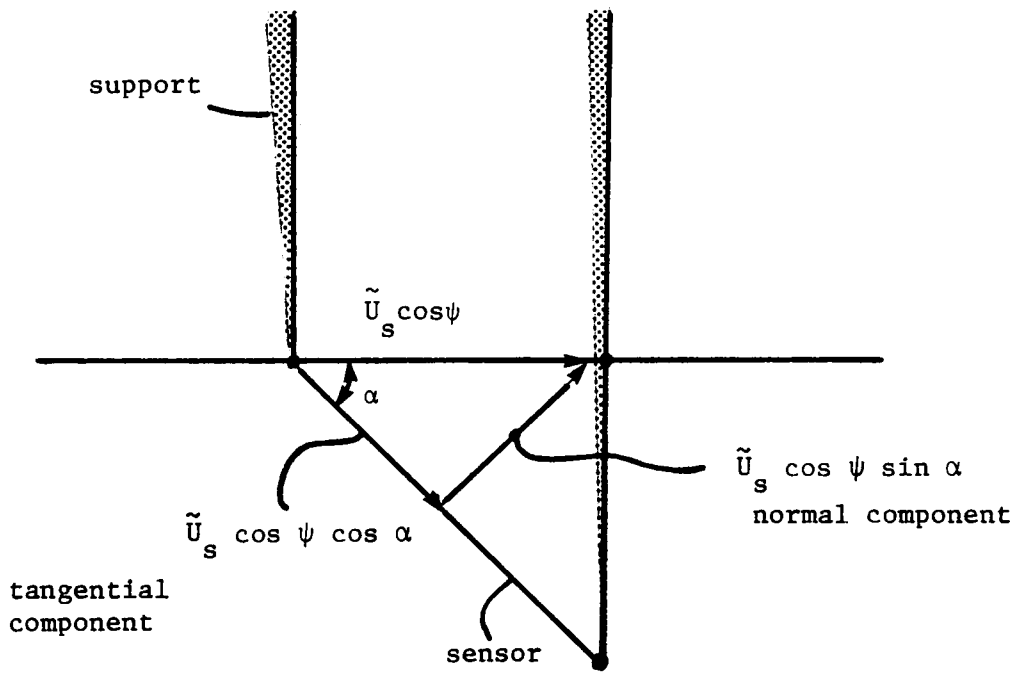

Figure 2.5 Decomposition of $\tilde{U}_s \cos\psi$ Velocity Component (from Fig. 2.4) in Vertical Plane Through Probe Supports

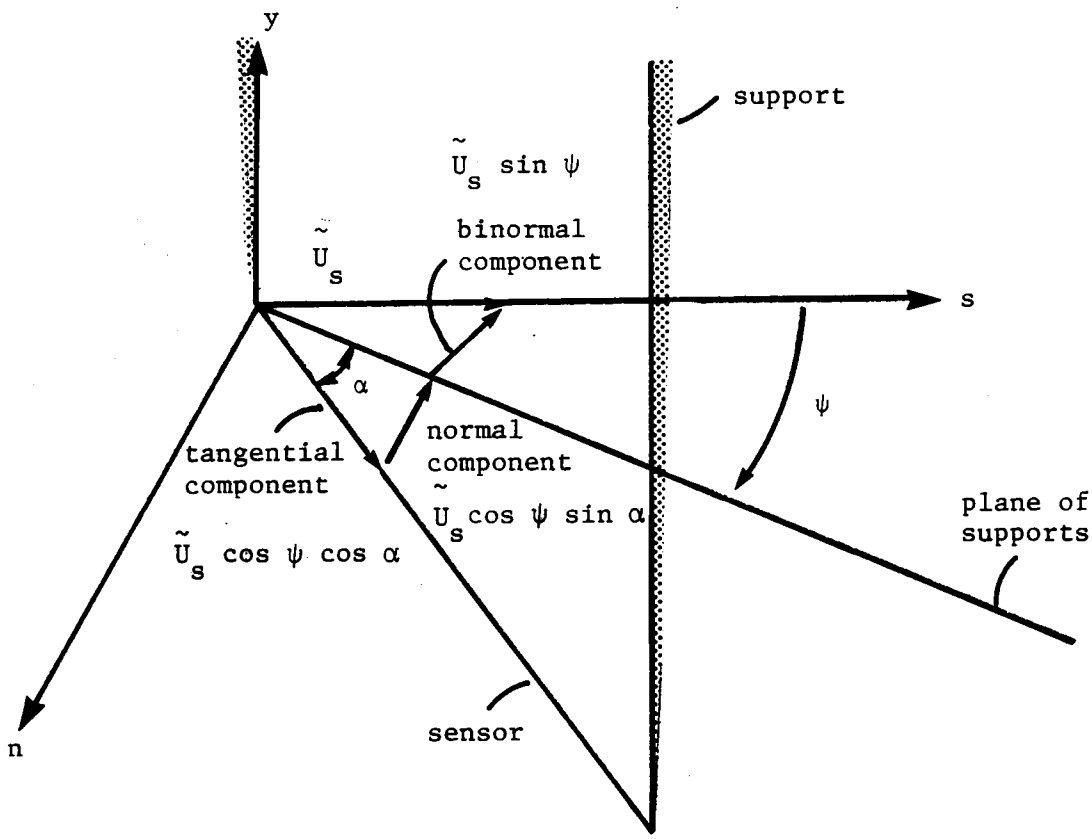

Figure 2.6 $\tilde{U}_s$ Velocity Component Decomposition
(Isometric View of Figs. 2.4, 2.5)

2.2.2.2 Decomposition of y Velocity Components

Next, the y component of velocity depicted in Figs. 2.7 and 2.8 is decomposed into T and N components, all in the same vertical plane of the wire supports.

$$- \tilde{U}_{y,T} = \tilde{U}_y \sin \alpha \tag{2.5}$$

$$\tilde{U}_{y,N} = \tilde{U}_y \cos \alpha \tag{2.6}$$

2.2.2.3 Decomposition of n Velocity Component

Last, the $\tilde{U}_n$ component is treated. Note that its mean value is zero by definition, but it can still have an instantaneous value due to turbulent fluctuations. In Fig. 2.9, the $\tilde{U}_n$ component is shown in its horizontal plane and broken into a BN component and a remainder. In Fig. 2.10, the remainder is depicted in its vertical true length plane coincident with the probe supports, and broken into T and N components. Refer to Fig. 2.11 for an isometric view.

$$- \tilde{U}_{n,BN} = \tilde{U}_N \cos \phi \tag{2.7}$$

$$\tilde{U}_{n,T} = \tilde{U}_N \sin \phi \cos \alpha \tag{2.8}$$

$$\tilde{U}_{n,N} = \tilde{U}_N \sin \phi \sin \alpha \tag{2.9}$$

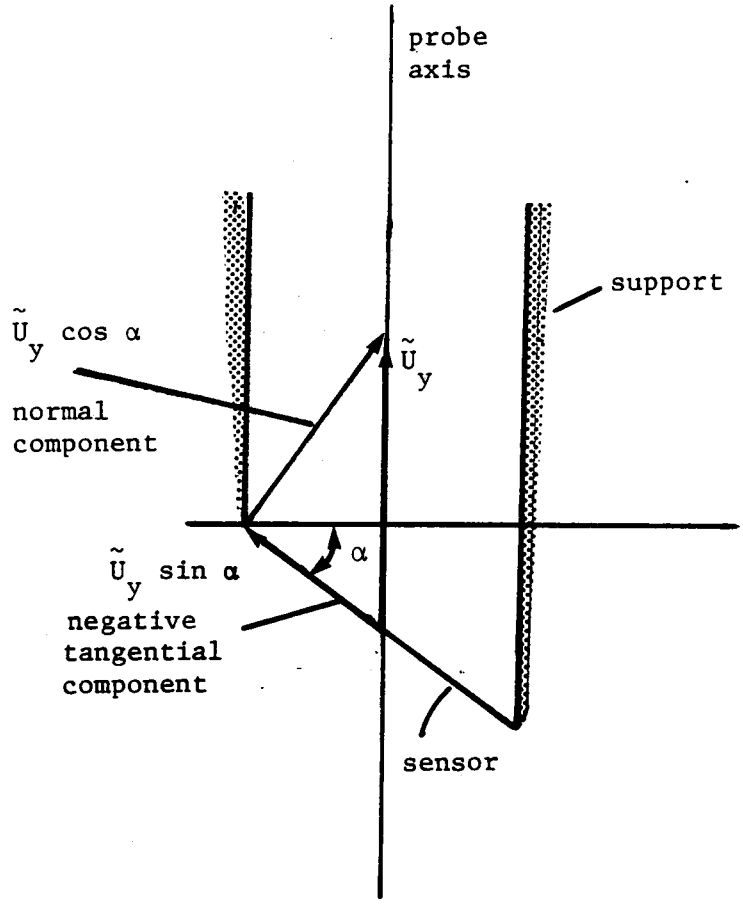

Figure 2.7 Decomposition of $\tilde{U}_y$ Vertical Velocity Component in the Plane of the Supports

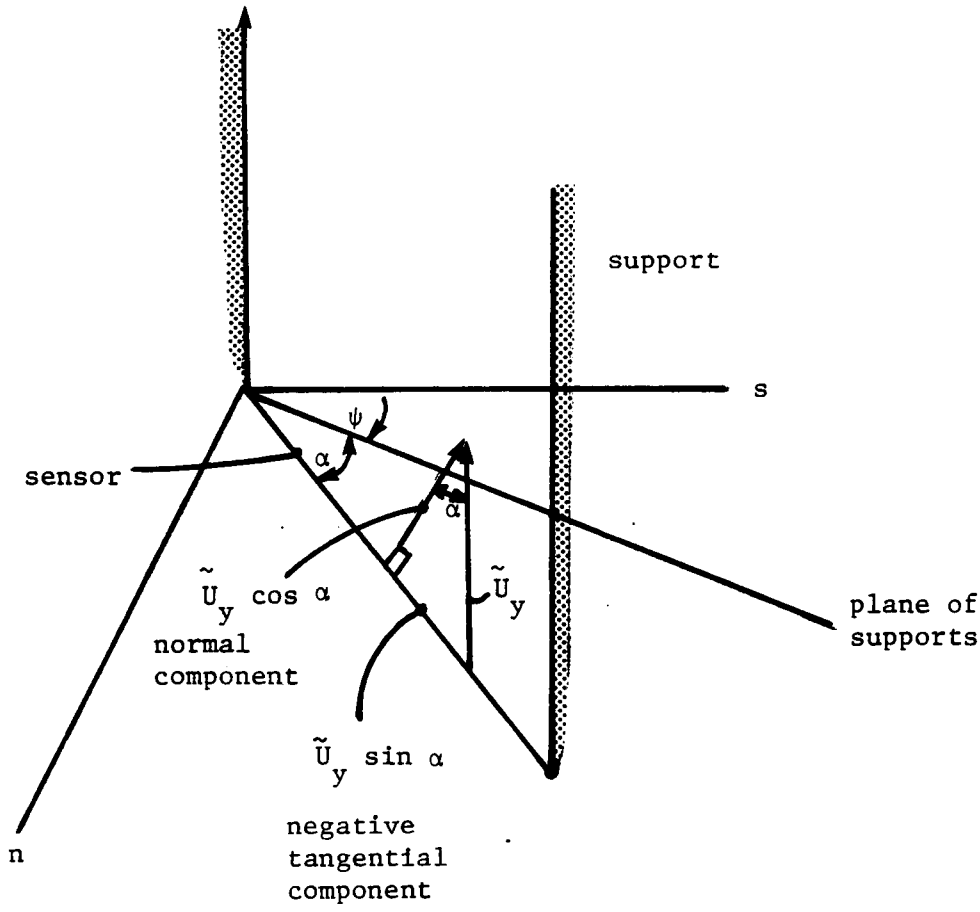

Figure 2.8 $\tilde{U}_y$ Velocity Component Decomposition
(Isometric View of Fig. 2.7)

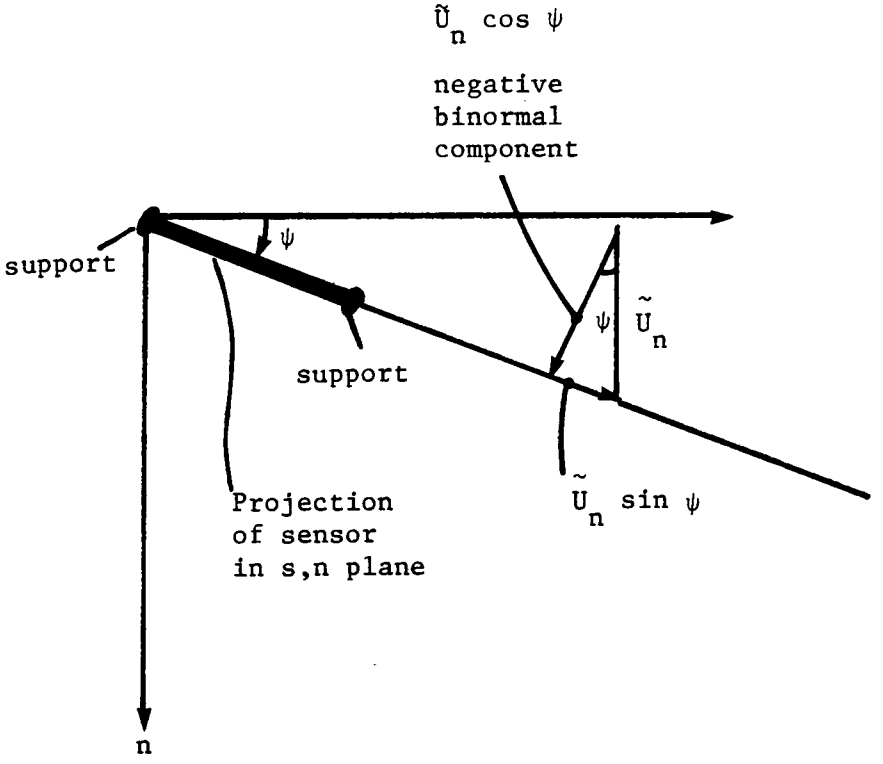

Figure 2.9 Decomposition of $\tilde{U}_n$ Velocity Component in the s,n Horizontal Plane

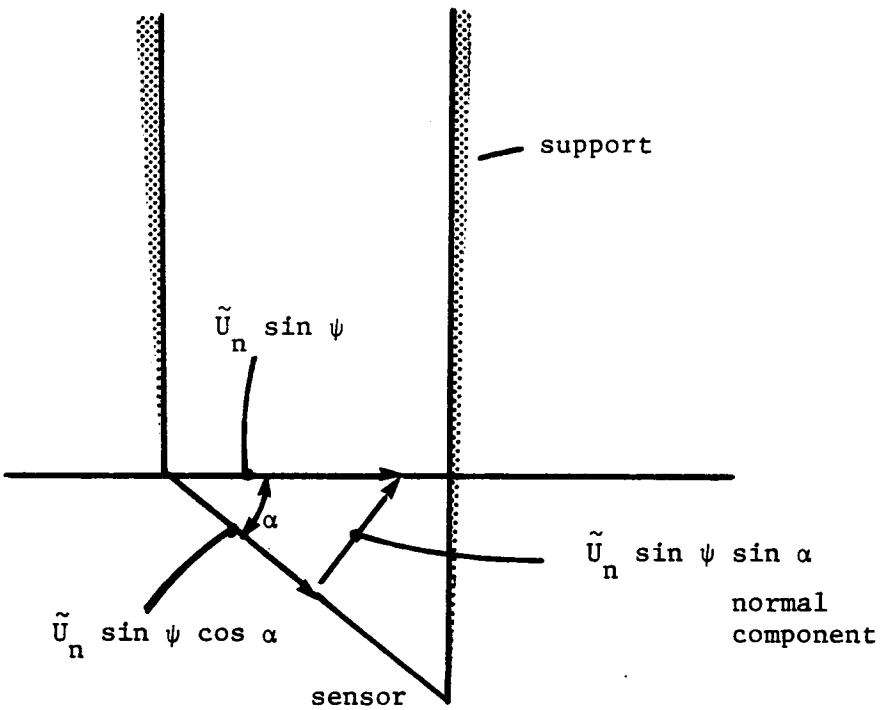

Figure 2.10 Decomposition of $\tilde{U}_n \sin \psi$ Velocity Component (from Figure 2.9) in the Vertical Plane through the Probe Supports

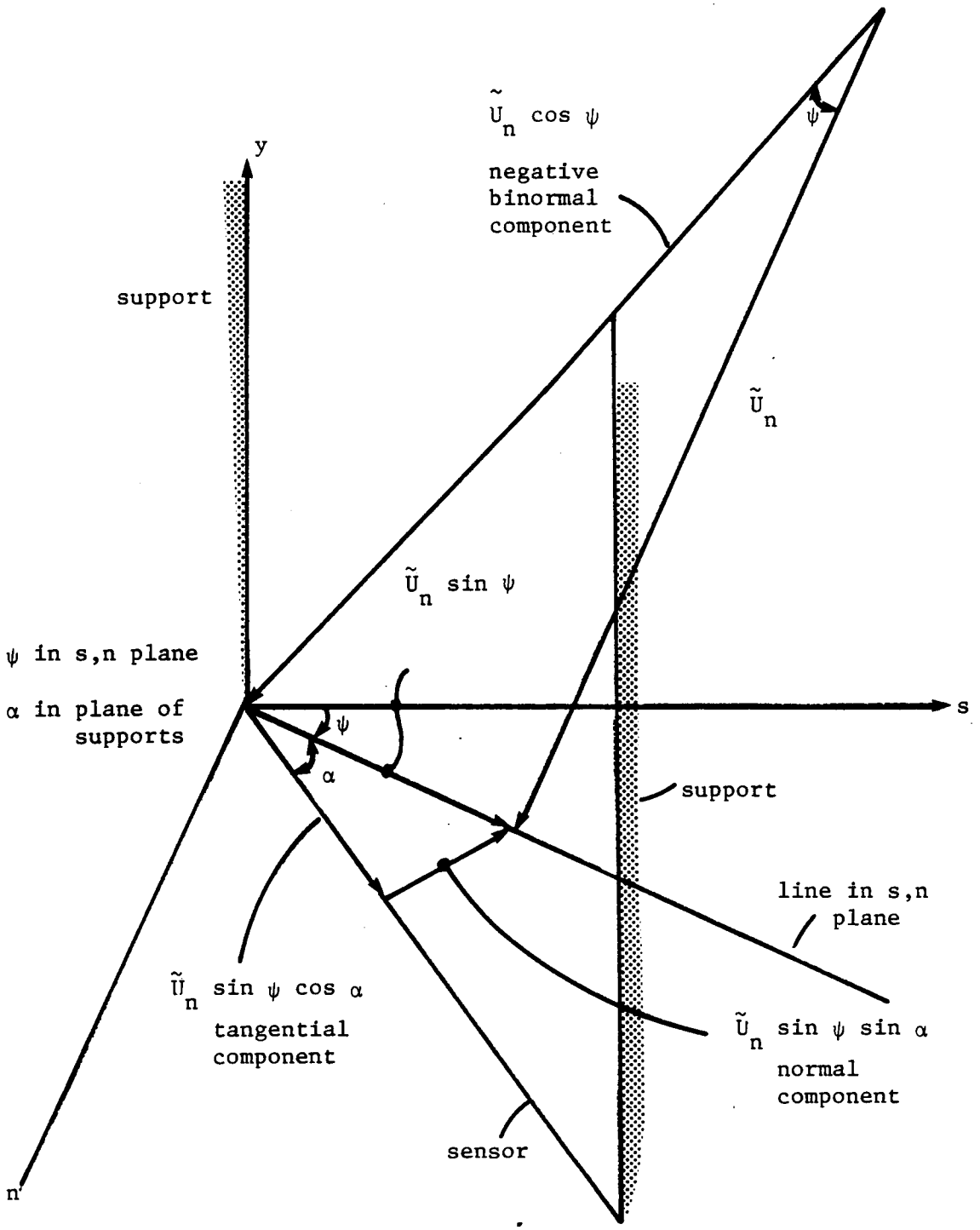

Figure 2.11 $\tilde{U}_n$ Velocity Component Decomposition
(Isometric View of Figs. 2.9, 2.10)

2.2.2.4 Composition of N,BN, T Components and Formation of Effective Velocity

The total U_N, U_{BN}, U_T components follow by adding their individual constituents from U_s, U_y, and U_n. These are signed quantities depending on their directional orientation.

$$\tilde{U}_N = [(U_s + u_s) \cos \phi + u_n \sin \phi] \sin \alpha + (U_y + u_y) \cos \alpha \qquad (2.10)$$

$$\tilde{U}_T = [(U_s + u_s) \cos \phi + u_n \sin \phi] \cos \alpha - (U_y + u_y) \sin \alpha \qquad (2.11)$$

$$\tilde{U}_{BN} = [(U_s + u_s) \sin \phi - u_n \cos \phi] \qquad (2.12)$$

Equations 2.10, 2.11, and 2.12 may be substituted into the Jorgenson cooling law, Eq. 2.1. Note that instantaneous values $\tilde{U}$ are expressed in terms of a mean value U and an instantaneous additional component u. Since U_n is zero, it has been omitted.

$$\tilde{U}_{eff}^2 = \{[(U_s + u_s)\cos \phi + u_n \sin \phi]\sin \alpha + (U_y+u_y)\cos\alpha\}^2$$

$$+ k^2\{[(U_s+u_s)\cos \phi + u_n \sin \phi]\cos\alpha - (U_y+u_y)\sin\alpha\}^2$$

$$+ h^2\{ (U_s + u_s) \sin \phi - u_n \cos \phi\}^2 \qquad (2.13)$$

2.3 Formation of General Response Equations

Consider the equation for linearized hot wire anemometer response:

$$\tilde{E}_\ell = S\,\tilde{U}_{eff} \tag{2.14}$$

$\tilde{E}_\ell$ may be expanded into a mean and a time variant component, E_ℓ and e_ℓ, respectively. $\tilde{U}_{eff}$ may be expanded in a similar way. Note that $E_\ell = \overline{E}_\ell$ and $U_{eff} = \overline{E}_{eff}$, and the overbar is included in the following to emphasize the average value.

$$\tilde{E}_\ell = E_\ell + e_\ell = S\tilde{U}_{eff} = S(U_{eff} + u_{eff}) \tag{2.15}$$

Taking the mean,

$$\frac{\overline{E_\ell}}{S} = \overline{U_{eff}} \tag{2.16}$$

Squaring Eq. 2.15 and taking means results in

$$\frac{\overline{E_\ell^{\,2}}}{S^2} + \frac{\overline{e_\ell^{\,2}}}{S^2} = \overline{\tilde{U}_{eff}^{\,2}} \tag{2.17}$$

Using Eq. 2.16, there results

$$\frac{\overline{e_\ell^{\,2}}}{S^2} = \overline{\tilde{U}_{eff}^{\,2}} - (\overline{U_{eff}})^2 \tag{2.18}$$

Equations 2.13, 2.16, 2.18 are the basis of the remainder of the analysis which yields general response equations for mean velocity components U_s, U_y and the six turbulent stresses $\overline{u_s^{\,2}}$, $\overline{u_y^{\,2}}$,

$\overline{u_n^2}$, $\overline{u_s u_y}$, $\overline{u_s u_n}$, $\overline{u_y u_n}$.

First, Eq. 2.13 for U_{eff} is expanded to yield U_{eff}^2 and $\overline{\tilde{U}_{eff}^2}$. The expanded expression may be put in the form

$$\tilde{U}_{eff} = U_s \sqrt{A_T} \; (1 + \varepsilon)^{1/2} \tag{2.19}$$

Note that U_s remains explicit in the main expression because its order of magnitude is assumed to be considerably larger than those of the other terms. Terms of third and higher order were neglected.

The term ε is given by the expression

$$\begin{aligned}\varepsilon = {} & \frac{2u_s}{U_s} + \frac{u_s^2}{U_s^2} + B_T\left[\frac{U_y^2}{U_s^2} + \frac{2U_y u_y}{U_s^2} + \frac{u_y^2}{U_s^2}\right] + \frac{C_T u_n^2}{U_s^2} \\ & - D_T\left[\frac{U_y}{U_s} + \frac{u_y}{U_s} + \frac{u_s U_y}{U_s^2} + \frac{u_s u_y}{U_s^2}\right] - E_T\left[\frac{U_y u_n}{U_s^2} + \frac{u_y u_n}{U_s^2}\right] \\ & + F_T\left[\frac{u_n}{U_s} + \frac{u_s u_n}{U_s^2}\right]\end{aligned} \tag{2.20}$$

A_T through F_T are given by

$$A_T = \cos^2\psi \sin^2\alpha + k^2\cos^2\psi \cos^2\alpha + h^2 \sin^2\psi \tag{2.21}$$

$$B_T = (\cos^2\alpha + k^2 \sin^2 \alpha)/A_T \tag{2.22}$$

$$C_T = (\sin^2\psi \sin^2\alpha + k^2\sin^2\psi \cos^2\alpha + h^2\cos^2\psi)/A_T \tag{2.23}$$

$$D_T = 2 \sin \psi \sin \alpha \cos \alpha \, (k^2 - 1)/A_T \tag{2.24}$$

$$E_T = 2 \sin \psi \sin \alpha \cos \alpha \, (k^2 - 1)/A_T \tag{2.25}$$

$$F_T = 2 \cos \psi \sin \psi \, (\sin^2\alpha + k^2\cos^2\alpha - h^2)/A_T \tag{2.26}$$

Next, Eq. 2.19 is expanded in a Taylor series and third and higher order terms are neglected to result in:

$$\tilde{U}_{eff} = U_s \sqrt{A_T} \left(1 + \frac{\varepsilon}{2} - \frac{\varepsilon^2}{8}\right) \tag{2.27}$$

Taking time averages of Eq. 2.27 results in

$$\overline{\tilde{U}_{eff}} = U_s \sqrt{A_T} \left(1 + \frac{\bar{\varepsilon}}{2} - \frac{\overline{(\varepsilon^2)}}{8}\right) \tag{2.28}$$

Squaring Eq. 2.28 results in

$$(\overline{\tilde{U}_{eff}})^2 = U_s^{\,2} \; A_T \left[1 + \bar{\varepsilon} + \frac{(\bar{\varepsilon})^2}{4} - \frac{\overline{(\varepsilon^2)}}{4}\right] \tag{2.29}$$

The time average of the square of Eq. 2.27 is as follows:

$$\overline{(\tilde{U}_{eff}^{\,2})} = U_s^{\,2} \; A_T \left(1 + \bar{\varepsilon}\right) \tag{2.30}$$

Equations 2.28, 2.29, and 2.30 are substituted into Eqs. 2.16 and 2.17 to yield:

$$\frac{\overline{E_\ell}}{S} = U_s \sqrt{A_T} \left(1 + \frac{\bar{\varepsilon}}{2} - \frac{\overline{(\varepsilon^2)}}{8}\right) \tag{2.31}$$

and

$$\frac{\overline{e_\ell^2}}{S^2} = \frac{U_s^2}{4} A_T[(\overline{\varepsilon^2}) - (\overline{\varepsilon})^2] \tag{2.32}$$

Ultimately, Eq. 2.20 is used to evaluate $\overline{\varepsilon}$, $(\overline{\varepsilon})^2$, and $(\overline{\varepsilon^2})$, with third and higher order terms dropped. After substitution of the expression for ε into Eqs. 2.31 and 2.32, there results

$$\frac{\overline{E_\ell}}{S} = U_s \sqrt{A_T}\ [1 + (\frac{B_T}{2} - \frac{D_T^2}{8})(\frac{U_y^2}{U_s^2} + \frac{u_y^2}{U_s^2}) - \frac{D_T}{2}\frac{U_y}{U_s} + (\frac{C_T}{2} - \frac{F_T^2}{8})\frac{\overline{u_n^2}}{U_s^2} - (\frac{E_T}{2} - \frac{D_T F_T}{4})\frac{\overline{u_y u_n}}{U_s^2}\ ] \tag{2.33}$$

and

$$\frac{\overline{e_\ell^2}}{S^2} = U_s^2 A_T[\frac{\overline{u_s^2}}{U_s^2} + \frac{D_T^2}{4}\frac{\overline{u_y^2}}{U_s^2} + \frac{F_T^2}{4}\frac{\overline{u_n^2}}{U_s^2} - D_T\frac{\overline{u_s u_y}}{U_s^2} - \frac{D_T F_T}{2}\frac{\overline{u_y u_n}}{U_s^2} + F_T\frac{\overline{u_s u_n}}{U_s^2}\ ] \tag{2.34}$$

Note that Eqs. 2.33 and 2.34 are referred to as the general response equations, and are the basis of the analysis which follows.

2.4 Specialization of General Response Equations for Mean Velocities and Turbulent Stresses

The previous two general response equations (Eq. 2.33, 2.34) may be specialized to particular values of ϕ for the horizontal and slant probes to minimize data requirements in solving for the two mean

velocities and six turbulent stresses. A basic assumption in specializing these equations is that k and h are taken as constants.

1) $\overline{u_s^2}$ is evaluated from Eq. 2.34 for the horizontal (α=0°) probe at an angle of ϕ=90° to yield

$$\frac{\overline{e_\ell^2}}{S^2}(90) = h^2\,\overline{u_s^2} \tag{2.35}$$

2) $\overline{u_y^2}$ and $\overline{u_s u_y}$ follow from Eq. 2.34 for the slant probe ($\alpha \approx 45°$) with ϕ=0° and 180° to yield

$$\frac{\overline{e_\ell^2}}{S^2}(0) + \frac{\overline{e_\ell^2}}{S^2}(180) = 2(\sin^2\alpha + k^2\cos^2\alpha)\cdot$$

$$\left[\overline{u_s^2} + \frac{(1-k^2)^2\sin^2\alpha\cos^2\alpha}{(\sin^2\alpha + k^2\cos^2\alpha)^2}\,\overline{u_y^2}\right] \tag{2.36}$$

and

$$\frac{\overline{e_\ell^2}}{S^2}(0) - \frac{\overline{e_\ell^2}}{S^2}(180) = 4\,(k^2 - 1)\sin\alpha\cos\alpha\,\overline{u_s u_y} \tag{2.37}$$

3) U_y follows from Eq. 2.33 for slant probe ($\alpha \approx 45°$) at ϕ = 0° and 180°

$$\frac{\overline{E_\ell}}{S}(180) - \frac{\overline{E_\ell}}{S}(0) = 2\,\frac{(1-k^2)\sin\alpha\cos\alpha}{(\sin^2\alpha + k^2\cos^2\alpha)^{1/2}}\,U_y \tag{2.38}$$

4) $\overline{u_n^2}$ and $\overline{u_s u_n}$ follow from Eq. 2.34 for the horizontal probe at $\psi = \pm 45°$

$$\frac{\overline{e_\ell^2}}{S^2}(+45) + \frac{\overline{e_\ell^2}}{S^2}(-45) = (k^2 + h^2)\left[\overline{U_s^2} + \frac{(h^2-k^2)^2}{(h^2+k^2)^2}\overline{u_n^2}\right] \tag{2.39}$$

$$\frac{\overline{e_\ell^2}}{S^2}(+45) - \frac{\overline{e_\ell^2}}{S^2}(-45) = 2(k^2 - h^2)\overline{u_s u_n} \tag{2.40}$$

5) U_s is determined from Eq. 2.33 for the horizontal probe at $\psi = 90°$

$$\frac{\overline{E_\ell}}{S}(90) = \left[hU_s + \frac{1}{2h^2}\left(\frac{U_y^2}{U_s} + \frac{u_y^2}{U_s}\right) + \frac{k^2}{2h}\frac{\overline{u_n^2}}{U_s}\right] \tag{2.41}$$

6) $\overline{u_y u_n}$ is determined from Eq. 2.34 for the slant probe ($\alpha \approx 45°$) at $\psi = \pm 25°$

$$\frac{\overline{e_\ell^2}}{S^2}(-\psi) - \frac{\overline{e_\ell^2}}{S^2}(+\psi) = 4\cos\psi\sin\psi[\sin^2\alpha - k^2\cos^2\alpha - h^2] \cdot$$

$$\left[-\overline{u_s u_n} + \frac{(1-k^2)\cos\psi\sin\alpha\cos\alpha}{\cos^2\psi\sin^2\alpha + k^2\cos^2\psi\cos^2\alpha + h^2\sin^2\psi}\overline{u_y u_n}\right] \tag{2.42}$$

The choice of $\psi = \pm 25°$ does not reflect any advantages in simplification of these equations, but was established by MHK [1] through sensitivity studies, as being the position that gave the best results for turbulent stresses involving the n direction.

A computer program for consecutive solution of Eqs. 2.35 through

2.42 is given in Appendix B. Minimal data requirements are as follows:

Slant probe $\alpha \approx 45°$

$\overline{e^2}$ at $\phi = 0, \pm 25°, 180°$

E at $\phi = 0, 180°$

Horizontal probe $\alpha = 0$

$\overline{e^2}$ at $\phi = \pm 45°, 90°$

E at $\phi = 90°$

Note that the Eqs. 2.35 through 2.42 are solved consecutively and need not be considered in a simultaneous procedure.

2.5 Use of General Response Equations in a Regression Procedure

Another possibility for determination of mean velocities and turbulent stresses from the general response Eqs. 2.33 and 2.34 would be by using a regression analysis rather than to specialize those equations at certain positions.

A larger but arbitrary number of data points would be taken with the probe oriented at other additional yaw positions to the flow. The probe yaw angles (ϕ) and the corresponding voltages obtained would be inserted into Eqs. 2.33 and 2.34, and the turbulent stress quantities would be the unknown coefficients. A least squares regression method

would be used to determine these quantities, since there would be more simultaneous equations than unknowns.

2.6 Coordinate Transformation from s,y,n to x,y,z

The final step in the analysis is to perform a coordinate transformation of the mean velocities and turbulent stresses from local s,y,n to global x,y,z laboratory coordinates.

Turbulent stresses are pre-multiplied and post-multiplied by tensors [6] containing direction cosines between the two coordinate systems. The turbulent stress transformation is as follows:

$$\begin{vmatrix} u_{xx} & u_{yy} & u_{zz} \\ u_{yx} & u_{yy} & u_{yz} \\ u_{zx} & u_{zy} & u_{zz} \end{vmatrix} = T_T \begin{vmatrix} u_s u_s & u_s u_y & u_s u_n \\ u_y u_s & u_y u_y & u_y u_n \\ u_n u_s & u_n u_y & u_n u_n \end{vmatrix} T_T^{\,T} \qquad (2.43)$$

where

$$T_T = \begin{vmatrix} t_{xs} & t_{xy} & t_{xn} \\ t_{ys} & t_{yy} & t_{yn} \\ t_{zs} & t_{zy} & t_{zn} \end{vmatrix} = \begin{vmatrix} \cos\theta & 0 & -\sin\theta \\ 0 & 1 & 0 \\ -\sin\theta & 0 & \cos\theta \end{vmatrix}$$

and the elements t_{ij} are the cosines of the angles between the axes as denoted by their subscripts. Mean velocities are transformed by vector

products as follows:

$$U_x = U_s \cos\theta - U_n \sin\theta \tag{2.44}$$

$$U_z = U_s \sin\theta + U_n \cos\theta \tag{2.45}$$

3. ANEMOMETER THEORY AND USE

3.1 Review of Hot Wire/Film Anemometry

A hot-wire/film anemometer [7,8,9] probe consists of an electrically heated wire or film sensor that is inserted into a flow stream. As the flow passes the sensor, there is a convective cooling effect that increases with the speed of the fluid.

With a constant temperature instrument, the heating current is produced by a bridge circuit fitted with a servo-amplifier that responds to any change in resistance of the sensor due to changes in its temperature. Thus, the temperature of the sensor is held constant and the voltage across the bridge is related to the flow velocity.

3.1.1 Heat Transfer Relations for a Sensor

The idealized hot-wire/film performance is based on the model of a very long wire placed in a uniform flow perpendicular to the sensor.

The classical equation to describe the cooling in such a situation was developed by King and is presented by Hinze [7].

$$Nu = C_1 \, Pr + C_2 \, Pr \, Re^{0.50} \tag{3.1}$$

This expression is analytical in origin, but the constants are empirical and depend on the particular installation. Hinze [7] reports that similar relationships were also developed by Kramers, and by Collis and Williams, all revealing approximately the same linear relationship

between heat convection coefficient and the square root of the velocity in the Reynolds number.

3.1.2 Relationship between Flow Velocity and Anemometer Voltage Output

Note that in a steady state situation, the heat convected away from the wire must equal that produced by electrical heating,

$$I^2R = E^2/R = q \tag{3.2}$$

The resistance R may be approximated as a linear function of temperature over a small range such that for a heated wire

$$R_w = R_o\ [1 + \alpha(T_w - T_o)] \tag{3.3}$$

and for a wire at the fluid temperature

$$R_f = R_o\ [1 + \alpha(T_f - T_o)] \tag{3.4}$$

or combining these

$$T_w - T_f = (R_w - R_f)/\alpha\ R_o \tag{3.5}$$

In the above expressions, the subscript o corresponds to a reference temperature. Subscripts w and f correspond to the temperature of the heated wire and the surrounding fluid temperature.

Performing a heat balance and relating the result to Eq. 3.1,

$$Nu = \frac{hd}{k_f} = \frac{q\ d}{\pi d \ell (T_w - T_f)\ k_f} = A'' + B''\sqrt{U} \tag{3.6}$$

where A" and B" are empirical constants. Substituting from Eq. 3.5 into 3.6, there results

$$\frac{E^2}{R_w(R_w - R_f)} = \frac{\pi\ k_f\ \ell}{\alpha\ R_o}\left[A'' + B''\sqrt{U}\right] = A' + B'\sqrt{U} \tag{3.7}$$

where A' and B' are again empirical constants.

This is the basic relationship used to describe hot wire/film performance, although the expression is usually generalized to allow exponents of velocity which vary in a range of about 0.5 in accordance with actual calibration results. The equation then becomes:

$$E^2 = A + BU^n \tag{3.8}$$

Solving for U,

$$U = \left[\frac{E^2 - A}{B}\right]^{1/n} \tag{3.9}$$

3.2 Probe Calibration

Calibration of probes to determine the constants A, B, and n is done where the flow is quiescent, having zero turbulence intensity.

These probes must be oriented such that the axis of the sensor element is perpendicular to the flow, as depicted in Fig. 3.1 for both horizontal and slant probes.

3.2.1 Calibration Tunnel and Probe Positioning for Calibration

Figure 3.2 depicts the calibration tunnel in the internal flow lab. The rig on the calibration tunnel retains the probe and allows it to be pitched through an angle of +57° to -25° in the vertical plane of the tunnel centerline. This angle is denoted as ϕ and shown in Fig. 3.2. A protractor is mounted on the rig for measurement of this angle.

Also the probe may be yawed through 360° about its own axis. This angle is called β and is depicted in Fig. 3.2. It may be read from a dial on the support rod.

Referring again to Fig. 3.1 which depicts probe calibration positions, the calibration of the horizontal probe is done with $\phi = 0$ in Fig. 3.2, and β such that the sensor axis is perpendicular to the flow.

The slant probe is calibrated with $\phi = \alpha$, the angle that the normal to the sensor axis makes with the probe supports in their plane, and further, β is such that the sensor axis is perpendicular to the flow.

3.2.2 Calibration Procedures

Procedures for calibration of the probe in the bridge circuit are fully delineated in a DISA manual [10].

The nonlinear calibration curve may be fit to the form $E^2 = A + BU^n$ by either of two methods:

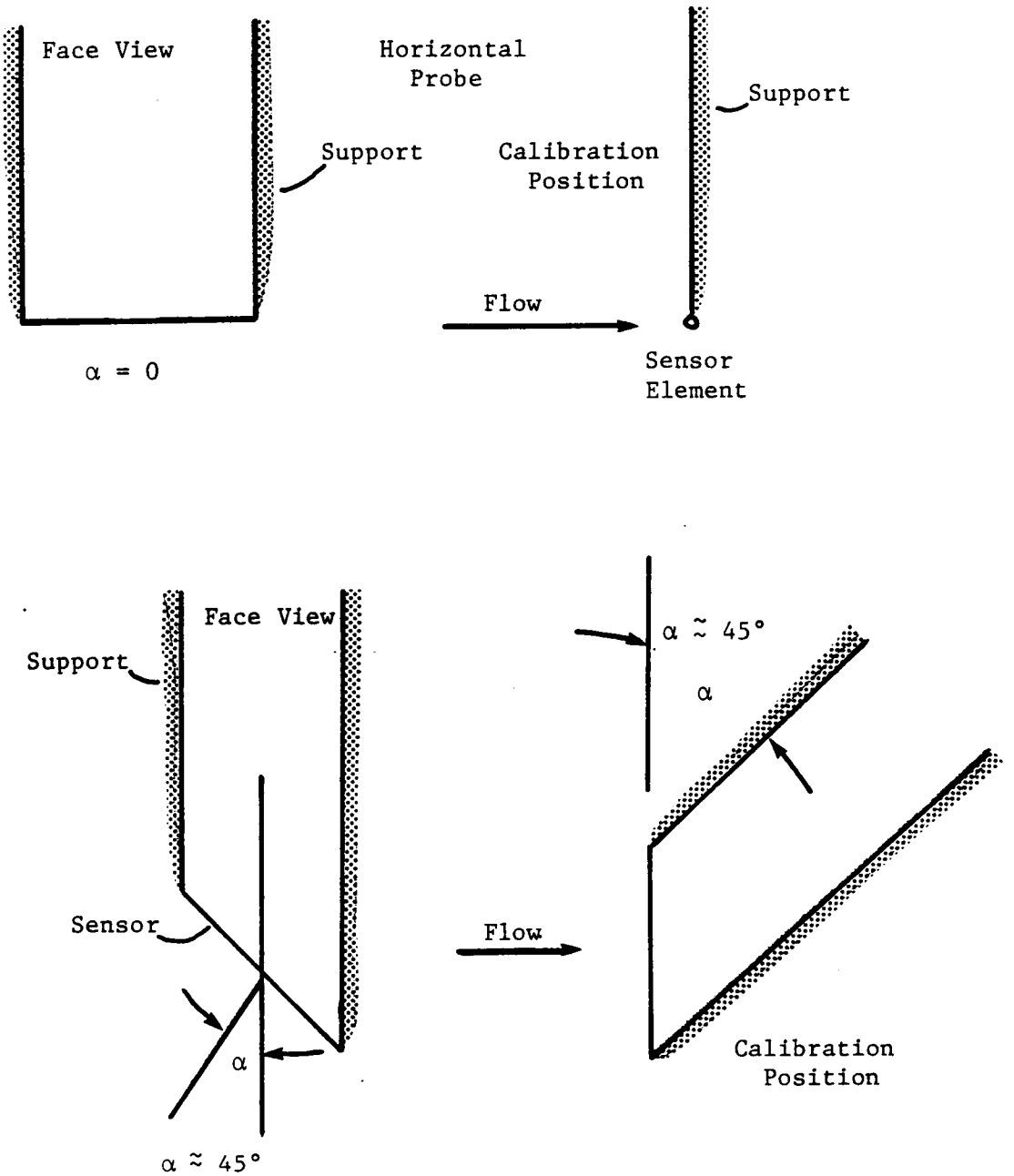

Figure 3.1 Probes in Calibration Positions

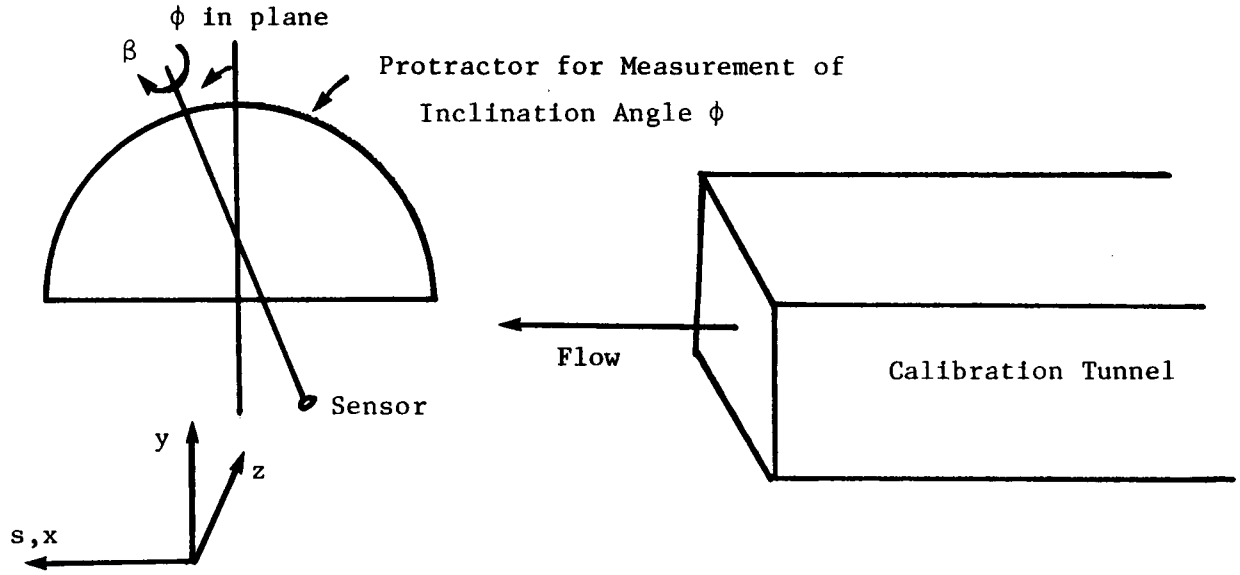

Fig. 3.2 Calibration Tunnel and Rig

1. The square of the zero velocity voltage is taken as A and subtracted from E^2. The variables $\ln(E^2-A)$ and $\ln U$ have a linear relationship with slope n and intercept $\ln B$ which may be determined by a linear least squares curve fit.
2. A nonlinear least squares curve fit may also be done to the form $E^2 = A + BU^n$ with the E vs U data. Three constants, A, B, and n are determined such that the best fit is obtained.

SAS regression programs are available to perform both of these methods of analysis on the computer.

3.2.3 Linearization and Signal Processing

Figure 3.3 shows a block diagram of the anemometer system. The bridge output voltage $E^2 = A + BU^n$ is often linearized such that at the linearizer output, the relationship $E_\ell = SU$ exists.

Basic steps in the linearizer calibration are summarized in the DISA literature [11].

Referring again to Fig. 3.3 it is seen that the linearizer output is fed in parallel to:

1) A digital voltmeter which filters out high frequency fluctuations, to facilitate getting a mean voltage output.
2) An rms meter followed by a digital voltmeter. The rms meter is dc coupled to block the mean value of the signal, and the rms of the fluctuations is passed as the output.

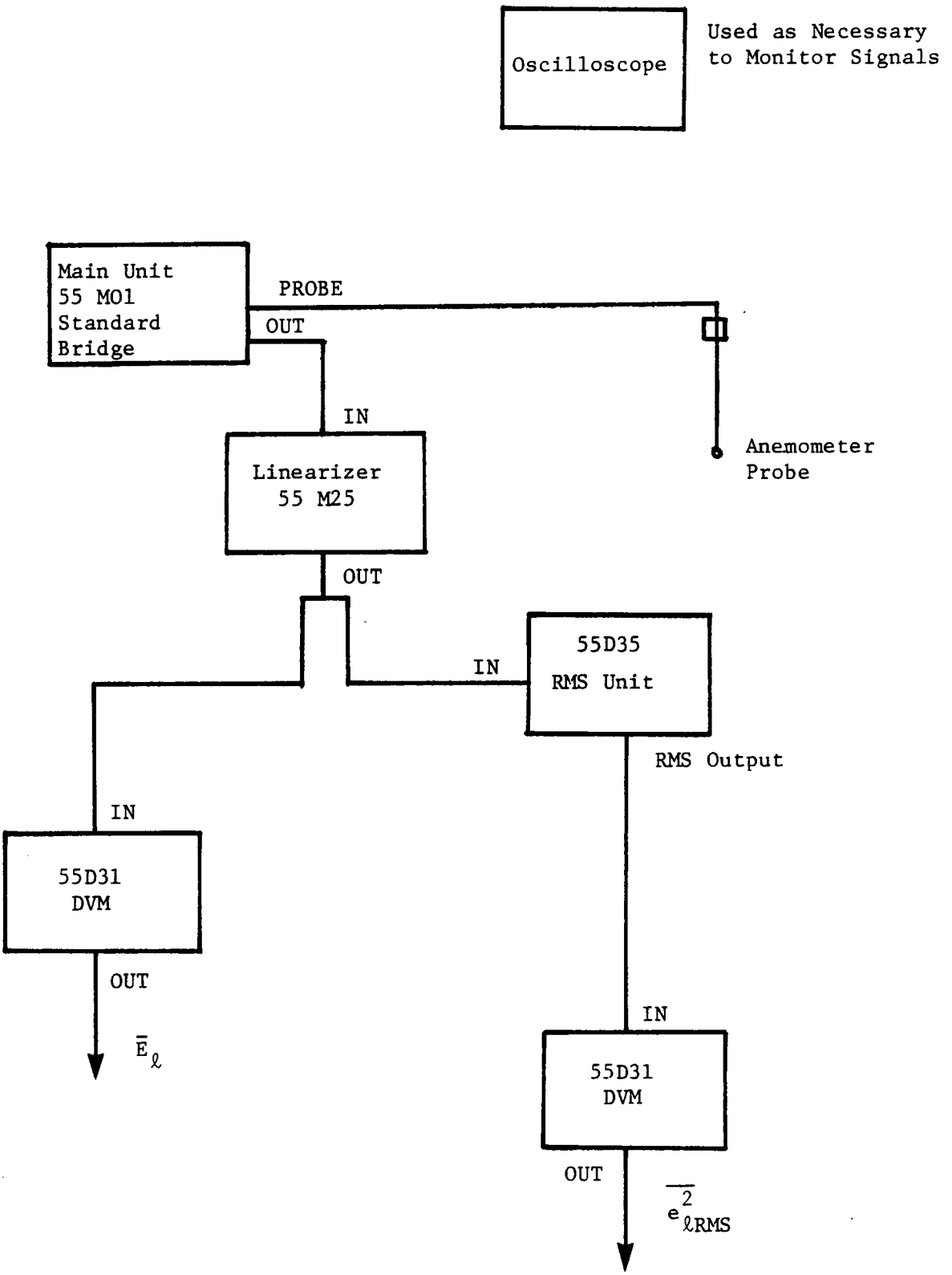

Figure 3.3. Block Diagram of Anemometer System

3.3 Jorgenson's Law for Effective Cooling Velocity

The basic anemometer performance equations as presented are based on an infinitely long sensor element placed in a flow field such that the axis of the sensor element is perpendicular to the flow velocity. No accounting was made for finite length and the presence of the probe supports, effects of which generally result in a flow direction sensitivity to the heat transfer from the sensor and the probe supports.

Obviously, in a three-dimensional flow field, the velocity may have in general any orientation to a sensor, and it may be expected that the cooling effect on the sensor may change accordingly.

3.3.1 Application of the Jorgenson Law

Jorgenson [12] has developed an expression for an effective velocity, U_{eff}, to be used in the basic anemometer performance equations in order to account for the directional characteristics of the probe-sensor element.

The expression is given as:

$$U_{eff}^2 = U_N^2 + k^2 U_T^2 + h^2 U_{BN} \tag{3.10}$$

U_{eff} is the effective velocity, and U_N, U_T, and U_{BN} are velocity components (as pictured in Figs. 2.2 and 2.3) relative to the sensor and probe. k and h are yaw and pitch coefficients that weight the velocity components according to their effectiveness in cooling the sensor. The quantities k and h will be taken as constants in this work even though

some authors [12] have noted that they may have a yaw and pitch dependence.

A distinction can be made between installation of the probe in end and cross flow configurations, which are depicted in Fig. 3.4.

Note that in the end flow configuration, the probe is placed in the flow such that the normal velocity component, U_N, is normal to the sensor and in the plane of the supports. The tangential component, U_T, is along the sensor. The remaining orthogonal component, U_{BN}, is normal to the sensor and perpendicular to the plane of the probe supports.

If this probe is now used in a cross flow configuration, the normal velocity component, U_N, is again normal to the sensor but now also normal to the plane of the sensor supports. The tangential component, U_T, is defined as before, along the sensor. The binormal velocity component, U_{BN}, is normal to the sensor but now in the plane of the sensor supports. The essential difference in the two orientations is that U_N and U_{BN} are interchanged, relative to the probe.

The Jorgenson law was originally proposed for end flow probes installations but is also applicable to cross flow installations; however, the velocities seen by the sensor and supports are different in the two configurations, and consequently the values of k and h differ for the same probe in end and cross flow installations.

The value of k is usually quite small [12] because the tangential component of velocity contributes little to the cooling effect on the sensor.

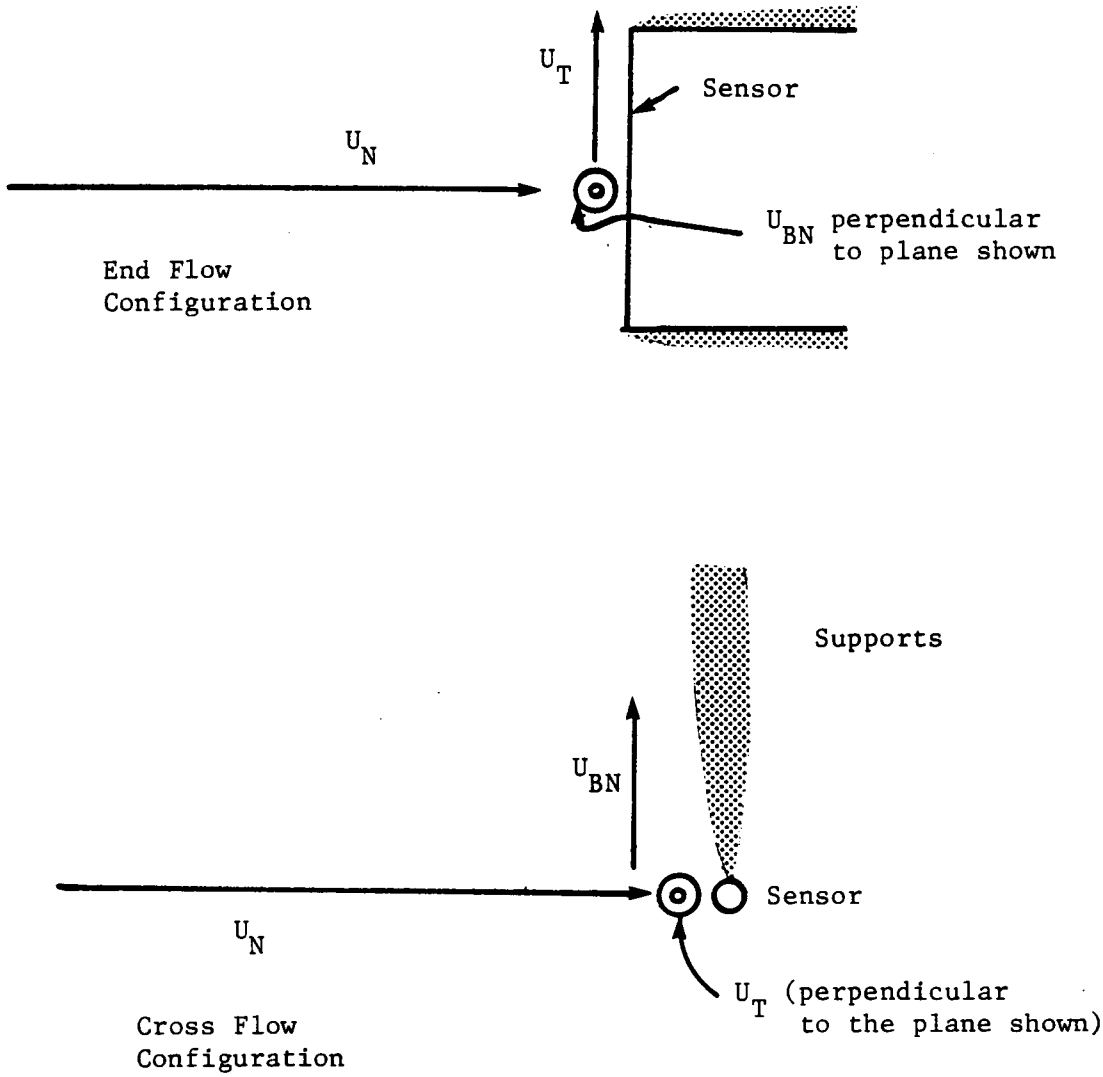

Figure 3.4 Illustration of Velocity Components on a Straight Single Sensor in End and Cross Flow Configurations

The value of h is usually close to 1.0 because of the relatively smaller effect which the sensor supports have, whether in end or cross flow configurations. The distinction between end and cross flow configurations is lost when h is assigned the value of 1.0 as done by MHK [1], and in this work, because the normal and binormal velocity components which are interchanged between end and cross flow both bear a coefficient of 1.0. Thus the equation may be used for either type of installation, but the value of k nevertheless is dependent on the end or cross flow configuration chosen, and must be measured accordingly.

3.3.2 Determination of Jorgenson k and h

Determination of Jorgenson k and h values is done after the basic calibration and linearization steps discussed in Section 3.2.2 and 3.2.3.

The k and h parameters are determined by calibration with the sensor yawed and pitched to a known flow.

Note that yaw and pitch of the probe, in general, are not the same as yaw and pitch of the sensor because these parameters are defined in terms of the principal axes of the sensor and probe, which are different for the slant probe. For a horizontal probe, the yaw and pitch of the probe and sensor are identical.

Frequently the yaw coefficient k is modeled as a function of the yaw angle of the sensor element relative to the flow direction. Similarly the pitch coefficient h can be modeled as a function of the pitch angle of the sensor element relative to the flow direction.

An analysis is presented in Appendix A to relate yaw and pitch of the sensor to the more directly measurable yaw and pitch of the probe.

For use in the MHK analysis, k and h are taken as constants. h is set equal to 1.0, and k is only measured with the probes at the specific positions at which the analysis requires data to be taken.

For the horizontal probe, k values are required at positions $\phi = \pm 45°$. k values obtained at $\pm 45°$ are averaged to get a single k value for use in either position.

For the slant probe, k value data is taken at $\phi = 0°$ and 180°. The k values obtained at $\phi = 0°$ and 180° are averaged because the MHK analysis only permits a single k value for all orientations. k values at $\phi = \pm 25°$ are assumed equal to this average value at 0 and 180°.

In the MHK alternate analysis in which the general response Eqs. 2.33 and 2.34 would be applied over a wider range of ϕ values and then regressed to determine turbulent stresses, there would be an opportunity to make use of improved accuracy using a more detailed calibration of k and h values as functions of yaw and pitch of the sensor to the flow. The analysis of Appendix A would be of use in this procedure.

3.3.2.1 Determination of k for the Horizontal Probe

Refer to Fig. 3.5 where the horizontal probe is shown rotated about the probe axis such that the sensor element makes an angle of 45° with the flow velocity in the calibration tunnel. Values of the voltage at $\pm 45°$ may be averaged for the determination of a single k_{45} value. The Jorgenson expression becomes

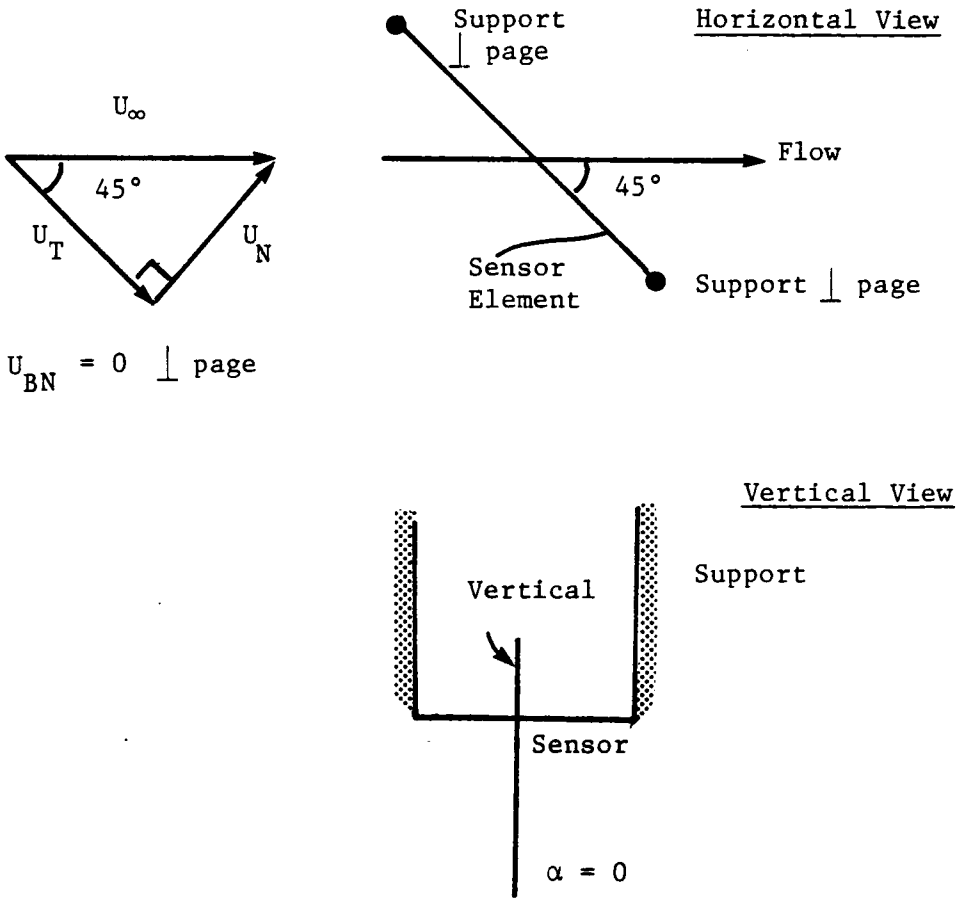

Figure 3.5 Illustration of Horizontal Probe Positioned at 45° to Flow for Determination of Jorgenson k

$$U_{eff(45)}^2 = k_{45}^2 U_T^2 + U_N^2 \tag{3.11}$$

where k_{45} is the Jorgenson k value with the sensor inclined at 45° yaw to the flow, and per the geometry of Fig. 3.5

$$U_{eff(45)}^2 = U_\infty^2 (k_{45}^2 \cos^2 45° + \sin^2 45°) \tag{3.12}$$

To relate this expression to the voltages measured in the laboratory with the sensor in the calibration position of Fig. 3.1 and oriented to the flow as in Fig. 3.5 we substitute in the following relations for linearized anemometer performance

$$E_{45} = S\ U_{eff\ 45} \tag{3.13a}$$

$$E_{fp} = S\ U_\infty. \tag{3.13b}$$

where the fp subscript denotes that the sensor element presents its full length to the flow as in the anemometer calibration position discussed in Section 3.2.1.

Solving for k_{45} there results

$$k_{45}^2 = \frac{(E_{45}/E_{fp})^2}{\cos^2 45°} \tag{3.14}$$

3.3.2.2 Determination of k for the Slant Probe

Figure 3.6 shows the slant probe at the $\psi = 0°$, 180° positions as defined in Fig. 2.1. Note that there is no normal component; therefore, the Jorgenson law for the 0° position becomes:

$$U_{eff} = U_{BN}^{2} + k_o^{2} U_T^{2} \tag{3.15}$$

where k_o is the Jorgenson k value for the slant probe with $\psi = 0°$, and making use of the trigonometric relationships depicted,

$$U_{eff}^{2} = U_\infty^{2} [\cos^2 \alpha + k_o^{2} \sin^2 \alpha] \tag{3.16}$$

This may be solved for k_o

$$k_o^{2} = \left(\frac{U_{eff}^{2}}{U_\infty^{2}} - \cos^2 \alpha\right)/\sin^2 \alpha \tag{3.17}$$

For linearized anemometer outputs,

$$E_o = SU_{eff} \tag{3.18}$$

and

$$E_{fp} = SU_\infty \tag{3.19}$$

Equations 3.14 and 3.15 are inserted into Eq. 3.13 to yield a relation for k in terms of voltages which can be measured with the probe oriented as indicated. There results:

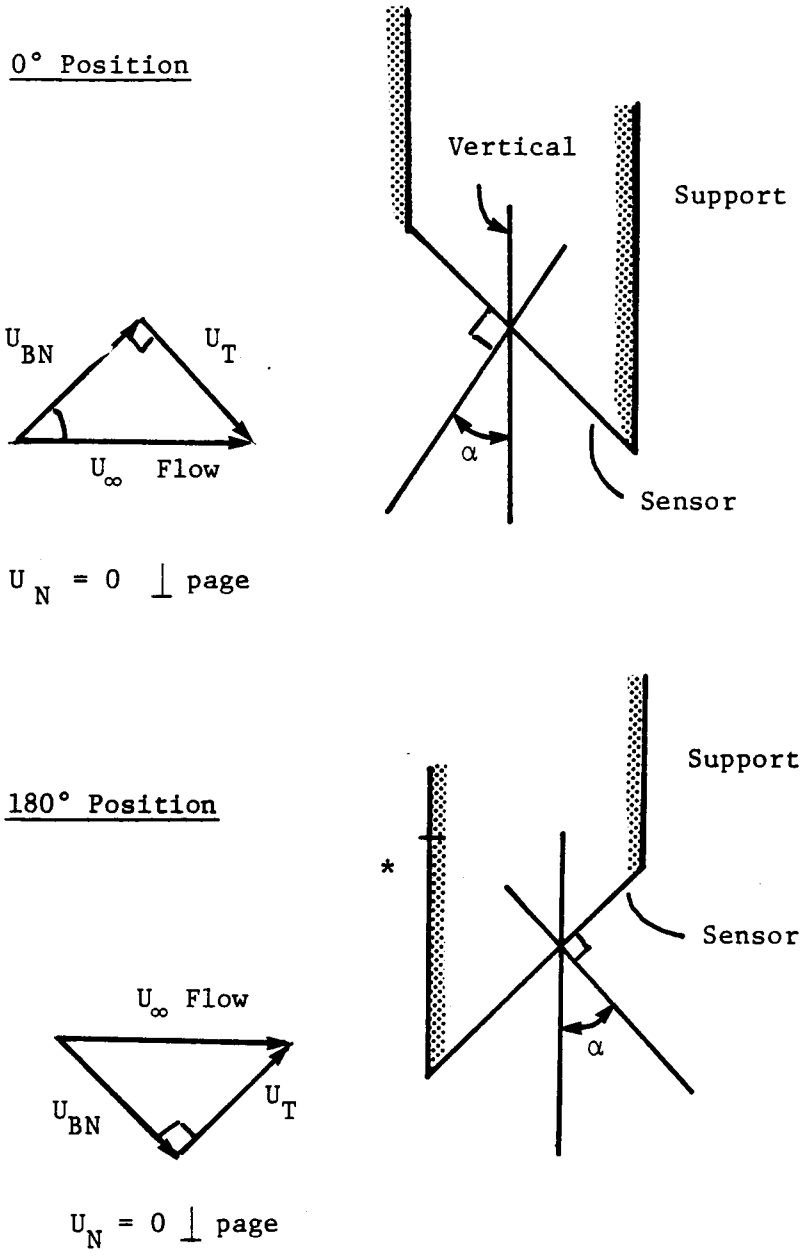

* Note that the longer support of the slant probe actually has a slight offset so that the sensor element is not in its wake at the $\psi = 180°$ position. (See also Fig. 2.3)

Figure 3.6 Illustration of Slant Probe with Probe Body Yaw of 0, 180° for Jorgenson k Determination

$$k_o^{\ 2} = \frac{[E_o/E_{fp}]^2 - \cos^2 \alpha}{\sin^2 \alpha} \tag{3.20}$$

An analogous development results in an equation for the value of k at the $\phi = 180°$ position which is:

$$k_{180}^2 = \frac{[E_{180}/E_{fp}]^2 - \sin^2 \alpha}{\cos^2 \alpha} \tag{3.21}$$

4. DESCRIPTION OF PHYSICAL SYSTEM

4.1. Tunnel and Instrumentation

The wind tunnel [13] is of open flow design. Flow is induced through an inlet section with a filter, screens, and straightening vanes, past the test section, through exit straightening vanes, and then exhausted by a 30 hp centrifugal fan with a discharge louvre for flow control. The test section has plexiglass™ siding with accessways, and a machined plate on the bottom for mounting of bodies.

The tunnel velocity is based on a reference throat unit Reynolds number of $Re = \rho U/\mu = 406{,}600/ft$. Air temperature is used in the Sutherland formula to determine viscosity

$$\mu = 7.14 \times 10^{-7} \frac{T^{1.5}}{T+180} \frac{lbm}{ft\ sec} \quad (T,\ ^\circ R) \tag{4.1}$$

The tunnel throat is fitted with a pitot static tube with a Datametrics digital micromanometer reading dynamic pressure.

4.2 Traverse System and Cathetometer

An automated traverse system [2] is located above the tunnel test section to hold and move the probes in the tunnel. The traverse has two degrees of freedom, vertical position and yaw angle. Motion is produced by stepping motors controlled by the data logger.

The horizontal position is established by moving the traverse as a unit. A vertical reference position of the probe is established with a cathetometer, which is essentially a telescope sight glass with leveling

and position adjustment mechanisms. The positioning of the probe must be done with the tunnel operating to account for small but real tunnel deflections. The cathetometer reticle is targeted to the top of a gage block placed on the tunnel floor. After removal of the block, the sensor is then moved to the same position viewed through the reticle. Any further movements are made in known distance increments until the sensor is at any desired vertical position.

4.3 Data Acquisition System

A Tandy Radio Shack TRS-80 Model III microcomputer [3,4,5] is used to control movements of the probe, the reading of various readout devices (typically digital voltmeters), and the recording of data. This is accomplished with a BASIC control program, and a machine language subroutine for the stepping motor control and movement.

4.3.1 Program Description

4.3.1.1 Required Inputs

The BASIC program initially prompts the operator in the set up of the system, allows initial vertical and yaw positioning of the probe, then requests manual input of data-taking parameters including:

1) Whether the profile shall be taken with the probe moving up or down.
2) Assignments of metering instruments to particular data acquisition channels in order that binary signal outputs may be properly decoded.

3) Vertical position schedule. A single traverse of the probe consists of sublengths called ranges, and each range is divided into equal steps. The number of ranges, number of steps per range, and step size must be input.

4) Choice of methods for aligning (nulling) the probe to the flow direction, usually a second order polynomial curve fit for anemometer probes, but this sequence can be bypassed for 2D profiles where direction is known and constant. The channel to be used in nulling, as well as yaw angle step size and range about the last null position must be specified to generate data for the curve fitting.

5) Time delays must be specified before the acquisition of data after the relocation of the probe, in order to allow equilibration of instrumentation to the new flow conditions. Also, it is necessary to specify the number of samples to be taken at a given probe position for each channel, and the time delay between sampling points.

6) Yaw position schedule. This allows the acquisition of data with the probe positioned at yaw angles deviating from the local streamline direction. Either individual deviations, or the total range about a streamline direction and the number of included points may be specified.

7) Initial reference positions for yaw and elevation must be specified.

8) The disk data file name must be specified for the storage of data.

4.3.1.2 Functioning of the Program During Data Acquisition

Functioning of the sequence is as follows for three dimensional flows.

At each elevation, the yaw angle is varied to find the null or local streamline direction. Anemometer output mean and rms voltage signal data is sampled, decoded, averaged, and stored for each channel. Next, voltage readings are taken with the anemometer sensor rotated to specific yaw positions relative to the local flow plane as required by the analysis.

The probe is moved to the next vertical position, and the sequence repeated.

4.3.2 Data Acquistion Hardware Functioning

Figure 4.1 depicts the complete data acquisition system as would be set up for data acquisition. A brief general description [2] of the computer interfacing follows.

Instructions to govern the proper operation of the digital data acquisition system pass from the BASIC program on the TRS-80 computer to an interface box through an external input/output bus. Three types of signals pass through the bus: control, address, and data signals.

Control signals are for sequencing and gating the data tansmission. Address signals allow selection of the proper device for input/output. The data signals contain the transmitted binary data such as digital voltmeter readings and pulse trains to stepping motors.

When movement of a stepping motor is required, the TRS-80 BASIC program determines the amount of movement required, calls the machine

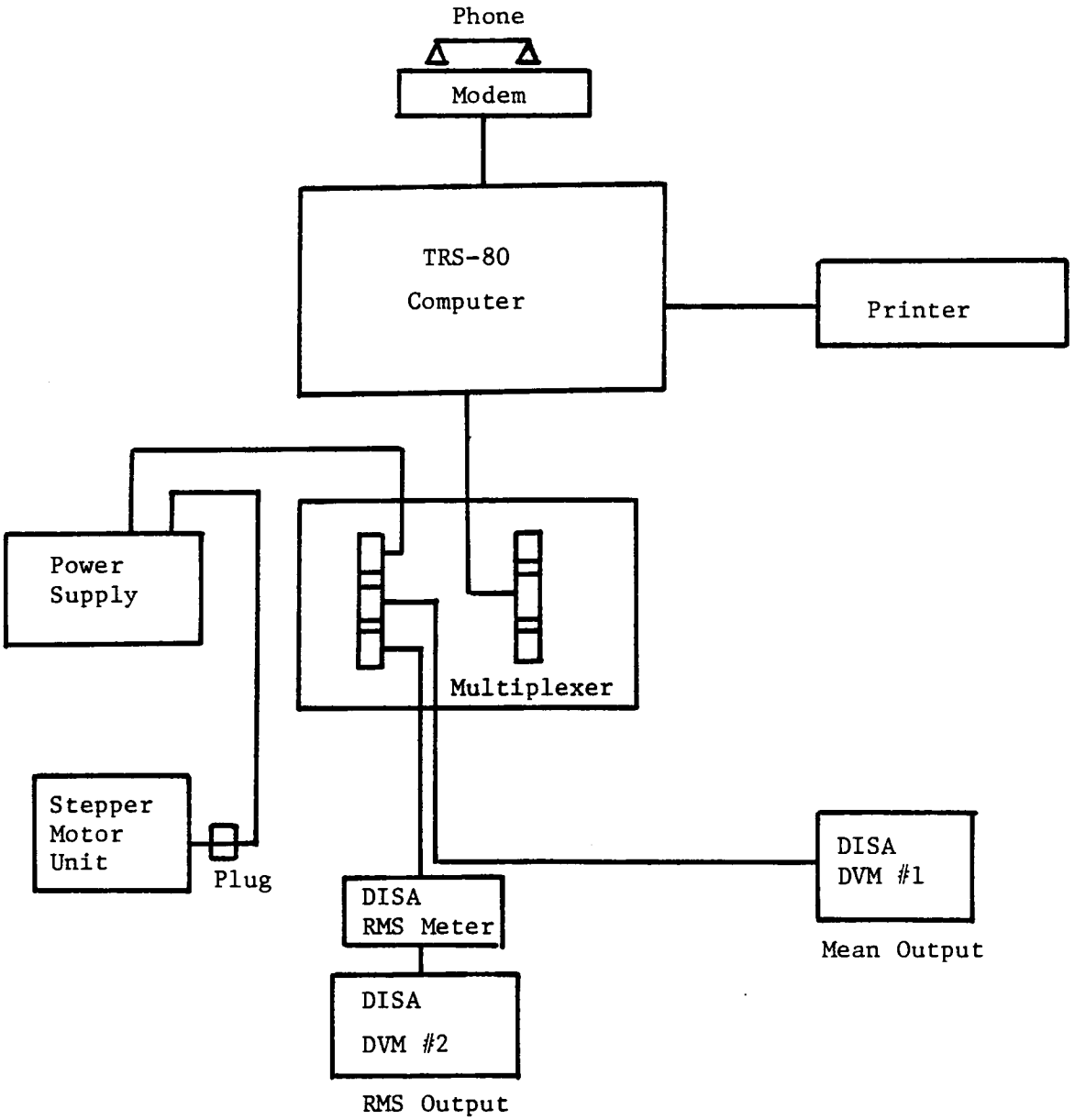

Figure 4.1 Block Diagram of Digital Data Acquisition System

language subprogram to generate the pulse train, and the pulses pass through the I/O signal ports on the bus together with an address signal to an interface box which acts as a multiplexer to enable the stepping motors to cause the required movements.

When it is time to read from a voltmeter, the computer sends an address signal to the multiplexer and the DVM output flows through the multiplexer to the computer for subsequent decoding according to its known compositional form. The resulting values are averaged and then written to a floppy disk for later use.

After all positions have been traversed and all data taken, data may be transferred by a modem unit through telephone line to an IBM mainframe computer from the floppy disk. A program is available to configure the TRS-80 computer as a smart terminal for this purpose. Data reduction is done on the mainframe.

4.3.3 Application of the Digital Data Acquisition System to the MHK Analysis

Note that at each horizontal location, a separate vertical traverse of the tunnel is made with the slant and with the horizontal probe. For each of these traverses, the program first prompts the operator to initialize parameters which govern the data acquisition, as described in Section 4.3.1.1. These parameters are all read onto the floppy disk for reference as to how the profile was taken.

Next, with the probe at its initial elevation, the yaw angle is ranged and the mean voltage data obtained is used in a second order polynomial curve fit to find an extremum which indicates the null or streamline direction. Generally at least thirty samples are taken of

each voltage signal at each position. Adequate delay times must be allowed between samples, and particularly after probe movement to allow equilibration of the system and the meters, in particular.

The elevation and null angle coordinate, θ, are read onto the floppy disk for subsequent use.

The probe is then returned to the null position and mean and rms voltages are sampled. Mean values and standard deviations are calculated and read to the floppy disk for both the mean and rms signals.

Next the probe is moved to the specific positions of yaw angle to the side of the local streamline direction, as required by the MHK analysis. Specifically, data is taken with the horizontal probe at $\phi = 90°, \pm 45°$. With the slant probe, data is taken at $\phi = 0°, \pm 45°, 180°$. Again, mean and rms voltages are sampled at these positions, and the mean values and standard deviations of the mean and rms signals are read to the floppy disk.

The data acquisition system functions during this process as described in Section 4.3.2.

When data has been taken at all required probe yaw angles, the microcomputer then activates the stepping motors to move the probe to a new elevation, where the procedure begins again from the point of nulling the probe. At completion of the slant and horizontal probe traverses, a separate data file exists on the floppy disk for each of the horizontal and slant probes. These are read into the mainframe computer through the telephone line, utilizing a modem unit connected to the microcomputer, which is configured as a smart terminal.

The new data files created on the mainframe computer may be accessed during the execution of the data reduction program. The data reduction programs on the mainframe include read statements which are programmed in the same sequence and format with which the data was stored on the floppy disk.

Thus, the initial contents of a data file is skipped as being a matter of record of parameters used in acquiring the data. Elevations, null angles, and mean and rms voltages corresponding to the specified angular positions are recognized according to their sequence by the mainframe for use in the reduction process.

5. EFFECTIVE APPLICATION OF THE SYSTEM AND ANALYSIS

Preliminary efforts were made to use the anemometer and data acquisition system. Experience gained in this preliminary work is summarized below for use of future users of the system.

Using Eq. 3.8 and the Jorgenson law (Eq. 2.1) applied to a horizontal and slant sensor pair, a nonlinearized analysis has been performed for determination of mean velocities and turbulent stresses in a two-dimensional boundary layer. A sensitivity analysis was then performed on this analysis using representative data from wires and films. Parameters entering these calculations were subjected to an arbitrary percentage change, and the corresponding percentage change in the turbulent stress quantities calculated was noted. These results are presented in Table 5.1 for wire probes, and Table 5.2 for film probes.

It can be readily seen that the anemometer calibration constants have an extremely severe effect on results obtained, being far more critical than any other parameter involved. Calibration must be done with great care.

These constants have a sensitivity to temperature and barometric pressure, which must be constant through the entire experiment to assure good results. Tunnel flow velocity may also drift and should be carefully controlled to preserve similarity in the flow field.

There can be a synergetic combination of errors when data from slant and horizontal probes are combined to calculate turbulent stresses. For example, the quantity $\overline{u_y u_y}$ in Eq. 2.36 is based on both slant probe voltages, and the $\overline{u_s u_s}$ value calculated from the horizontal probe data with Eq. 2.35.

Table 5.1 Sensitivity Study of Wire Probes with Two Dimensional Analysis

Quantity	Percent	Percent Change in Turbulent Stresses		
		Change		
		uu	vv	uv
K_o	+10	0	1.270	.920
K_o	-10	0	-1.251	- .895
K_{180}	+10	0	-5.289	5.868
K_{180}	-10	0	3.933	- 4.583
e^2rms(0°)	+ 5	0	16.697	12.969
e^2rms(0°)	- 5	0	-20.113	-12.970
e^2rms(180°)	+ 5	0	11.255	-13.566
e^2rms(180°)	- 5	0	-12.694	13.558
A_h	+ 5	- 3.538	14.266	- 6.480
A_h	- 5	3.110	-17.270	6.690
B_h	+ 5	- 9.471	37.893	-19.120
B_h	- 5	11.026	-59.683	24.660
N_h	+ 5	-21.083	69.834	-39.970
N_h	- 5	29.573	54.640	71.936
A_s	+ 5	0	-23.264	.700
A_s	- 5	0	19.429	- .735
B_s	+ 5	0	-71.448	1.070
B_s	- 5	0	54.744	- 1.393
N_s	+ 5	0	8.928	1.650
N_s	- 5	0	120.260	- 2.341

Table 5.2. Sensitivity Study of Film Probes with Two Dimensional Analysis

Quantity	Percent Change	Percent Change in Turbulent Stresses uu	vv	uv
K_o	+10	0	6.300	.840
K_o	-10	0	- .641	- .837
K_{180}	+10	0	- 1.266	2.023
K_{180}	-10	0	1.0355	- 1.688
$e^2rms(0°)$	+ 5	0	7.001	9.528
$e^2rms(0°)$	- 5	0	- 7.536	- 9.542
$e^2rms(180°)$	+ 5	0	4.430	- 7.324
$e^2rms(180°)$	- 5	0	- 4.643	7.310
A_h	+ 5	- 2.240	7.898	- 2.469
A_h	- 5	+ 2.236	- 8.769	2.500
B_h	+ 5	- 8.994	27.990	- 9.570
B_h	- 5	10.245	-56.895	12.190
N_h	+ 5	-21.162	55.095	-21.066
N_h	- 5	29.727	23.899	37.970
A_s	+ 5	0	-12.582	- 2.037
A_s	- 5	0	11.357	2.060
B_s	+ 5	0	-56.147	- 7.603
B_s	- 5	0	42.470	9.680
N_s	+ 5	0	-15.812	-16.532
N_s	- 5	0	100.000	29.480

Figure 5.1 shows a plot of anemometer output voltage versus probe yaw angle for the slant film sensor with $\phi = 0$. Because the sensor is inclined at 45° to the calibration tunnel flow in either of the $\phi = 0$ or 180° positions, it is to be expected that the voltages obtained in these two positions, and hence the Jorgenson k values, would not differ greatly. In fact, the Jorgenson k values were averaged at 0° and 180° positions to get the single k value required in the MHK analysis. Clearly this is not justified by the data of this figure, and would be expected to be a source of error.

Accuracy of determination of turbulent stresses is also dependent on the proper functioning of the anemometer hardware. Careful attention should be paid to internal calibration procedures before external calibration is done, and signals should be monitored occasionally on an oscilloscope as a function check.

One of the major goals of this effort was to establish the proper functioning of the digital acquisition system.

The system was observed to make movements in the proper sequence and magnitude. Meter readings were also determined to be accurately taken and decoded in the proper sequence. All calculations done by the system, such as polynomial curve fits for nulling, and statistical evaluation of data, were checked and verified. No problems are known to exist with the digital data acquisition system in its current state.

A problem had been suspected earlier of interference between the computer and the anemometer system, but investigations have eliminated this concern. The computer connection cable was lengthened so that the computer could be moved away further from the anemometer. Regardless of

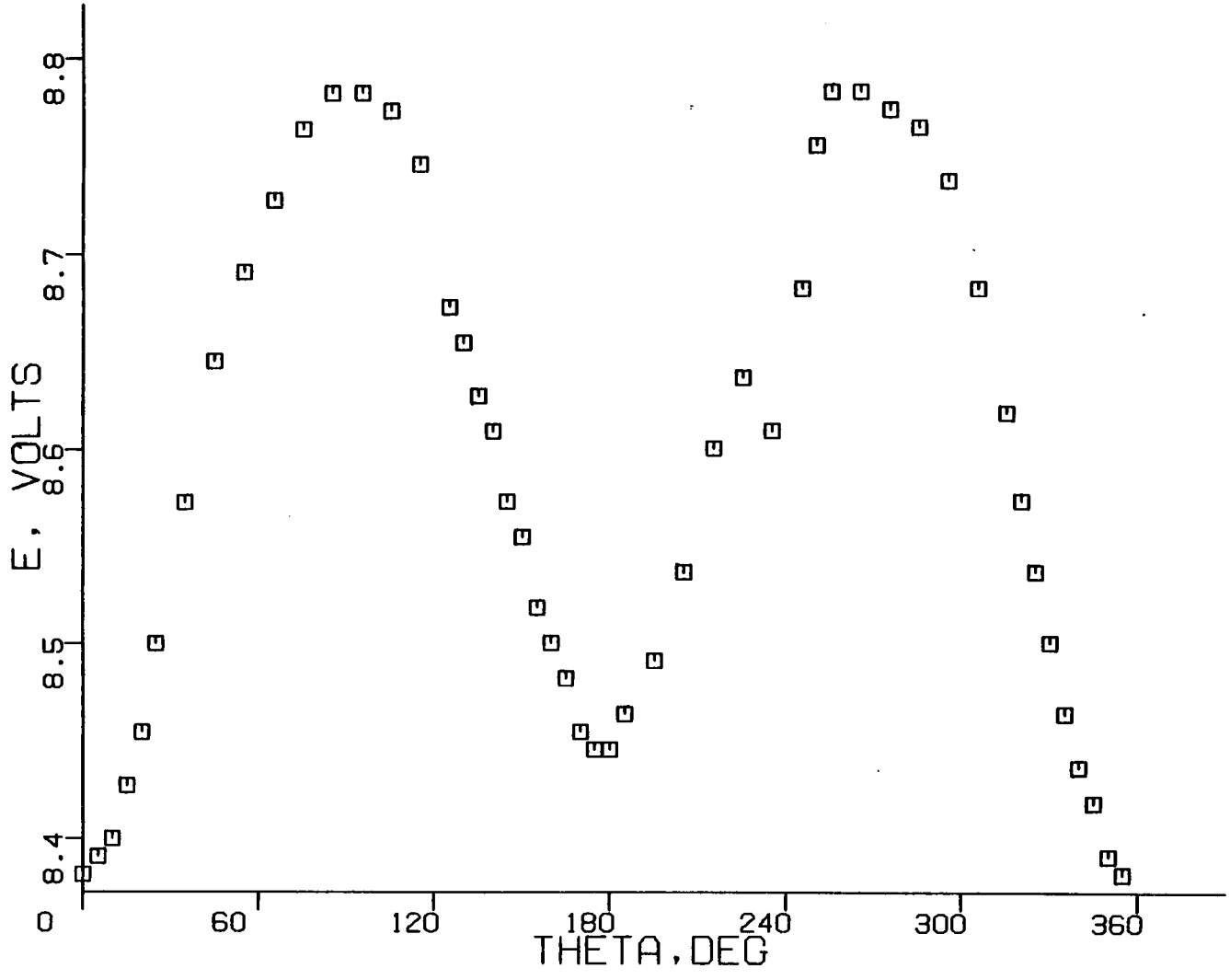

FIGURE 5.1
VOLTAGE VERSUS YAW ANGLE
FOR THE SLANT FILM PROBE

its distance, no change was seen either on the oscilloscope waveform or on the DVM displays. Turning the computer on or off also did not affect meter readings or waveforms.

In utilizing this digital data acquisition system, generous time delays must be allowed after moving the probe before acquisition of data, in order to allow stabilization of the system. At least one to two periods of integration of the rms meter should be allowed, as well as 4 to 5 DVM time constants to eliminate transient effects.

Meter integration periods and time constants should be as large as possible without prolonging traverse time extensively. This will insure that the full scale of turbulence is captured, as well as damping out any random trends in the signals measured.

Further, as mentioned earlier, at least 30 samples should be taken on each channel at each position to assure accuracy and precision of measurements.

6. SUMMARY

The hot wire/film anemometer analysis of McMahon, Hubbartt, and Kubendran [1] has been reviewed in detail for the measurement of mean velocities and turbulent stresses in a three dimensional flow field dominated by a streamwise mean velocity. This analysis uses a single slant and a single horizontal sensor element. A code has been developed to reduce data according to this analysis, and is presented in Appendix B.

The acquisition of data for use in this analysis is done with an automated traverse and digital data acquisition system, which has been modified specifically for this purpose. Details of this system and its operation to acquire data for the MHK analysis have been discussed.

Basic anemometer theory and use have been reviewed and applied to this specific application. In particular, the matter of calibration of probes has been treated in detail.

A special analysis is presented in Appendix A to relate yaw and pitch of the sensor to yaw and pitch of the probe.

Preliminary calibrations have been done, and tunnel data has been taken and reduced according to these analyses. Experience gained with the anemometer system and the digital data acquisition system has been summarized for the convenience of future users of the system.

REFERENCES

1. McMahon, H., J. Hubbartt, and L. Kubendran, "Mean Velocities and Reynolds Stresses in a Juncture Flow," NASA Contractor Report 3605, Grant NAG1-40, Langley Research Center, Aug. 1982.

2. Herwig, N. L., "Design of a Data Acquisition System to Control and Monitor a Velocity Probe in a Fluid Flow Field," M.S. Thesis, VPI&SU, December 1982.

3. Tandy Corp., Getting Started with TRS-80 BASIC, Cat. No. 26-2107, Fort Worth, TX, 1981.

4. Tandy Corp., TRS 80 Model III Operation & BASIC Language Reference Manual, Cat. No. 26-2112, Fort Worth, TX, 1980.

5. Tandy Corp., Model III Disk System Owner's Manual, Cat. No. 26-2111, Fort Worth, TX, 1980.

6. Mase, G. E., Continuum Mechanics, Schaum's Outline Series, McGraw-Hill, New York, 1970, pp. 49-50.

7. Hinze, J. O., Turbulence, McGraw-Hill, New York, 1959.

8. Bradshaw, P., An Introduction to Turbulence and its Measurement, Pergamon Press, New York, 1971.

9. Vagt, J. D., "Hot Wire Probes in Low Speed Flow," Progress Aerospace Science, Vol. 18, 1979, pp. 271-323.

10. DISA Electronics, "Type 55M10 Instruction Manual - DISA 55M System with 55M10 CTA Standard Bridge," DISA Information Department.

11. DISA Electronics, "Type 55M25 Linearizer Instruction Manual," DISA Information Department.

12. Jorgenson, F. E., "Directional Sensitivity of Wire and Fiber Film Probes," DISA Information Paper, Nov. 20, 1970.

13. Harsh, M. D., "An Experimental Investigation of a Turbulent Junction Vortex," Ph.D. dissertation, VPI&SU, January 1985.

APPENDIX A

Derivations of Expressions for Yaw and Pitch of the Sensor Element in Terms of Yaw and Pitch of the Probe

A.1 Introduction

Jorgenson k and h values are based on yaw and pitch of the sensor, but it is yaw and pitch of the probe that are directly measurable in the laboratory. Therefore, equations were developed to relate the yaw and pitch of the anemometer sensor element to the yaw and pitch of the probe body, in order that k and h could be determined as functions of sensor yaw and pitch for use in the analysis of Section 2.5.

A.2 Coordinate System Description

The analysis which follows will be based on the most general case which exists in this experiment, which is the case of the probe holder rig on the calibration tunnel.

The calibration tunnel coordinates are depicted in Fig. A.1. Yaw and pitch of the probe are given as β and ϕ, as shown.

A.3 Determination of Yaw and Pitch of the Sensor

Yaw of the sensor may be defined as the angle that the sensor element makes with the local mean velocity vector.

Pitch of the sensor may be described as the rotation of the probe about the sensor element axis.

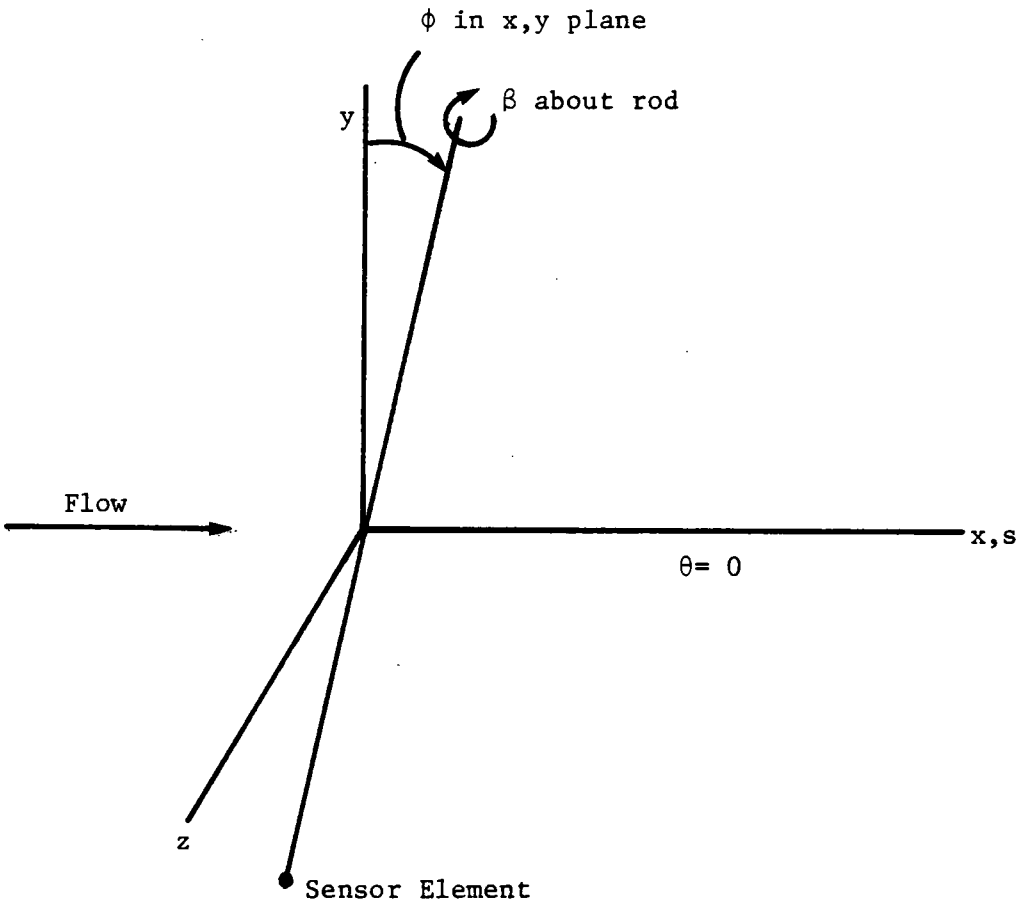

Figure A.1 Illustration of Probe Yaw β and Pitch ϕ

Steps in the determination of sensor yaw and pitch are as follows:

First, a vector must be determined in x,y,z coordinates for the sensor element. It will be taken as the vector from the longer or reference support. Next the local velocity vector will be decomposed into x,y,z components. A unitized dot product of the two vectors yields the cosine of the angle that the element makes with the local velocity vector. This angle is the yaw of the sensor.

Next, the velocity is decomposed into supernormal and tangential components, and the supernormal component is further decomposed into normal and binormal components. The plane of the sensor supports is defined by a vector cross product between the sensor element and the supports. A definition of sensor pitch then follows from the angle between the normal to the plane of the supports, and the supernormal velocity component.

A.3.1 Determination of x,y,z Coordinates of the Sensor Element End

Consider first a slant probe projected into the x,y plane with $\phi = \beta = 0$ per Fig. A.2. The sensor element has components along the x and y axes of $\ell \cos\alpha$ and $\ell \sin\alpha$, respectively. If β is varied, $\ell \sin\alpha$ does not change its projection on y, but $\ell\cos\alpha$ projects as $\ell \cos\alpha \cos\beta$ on x. Adding also variation in β, the following is obtained:

$\ell \sin\alpha$ projects as $\ell \sin\alpha \cos\phi$ on y
as $\ell \sin\alpha \sin\phi$ on x

$\ell \cos\alpha \cos\psi$ projects as $\ell \cos\alpha \cos\beta \cos\phi$ on x
as $\ell \cos\alpha \cos\beta \sin\phi$ on y

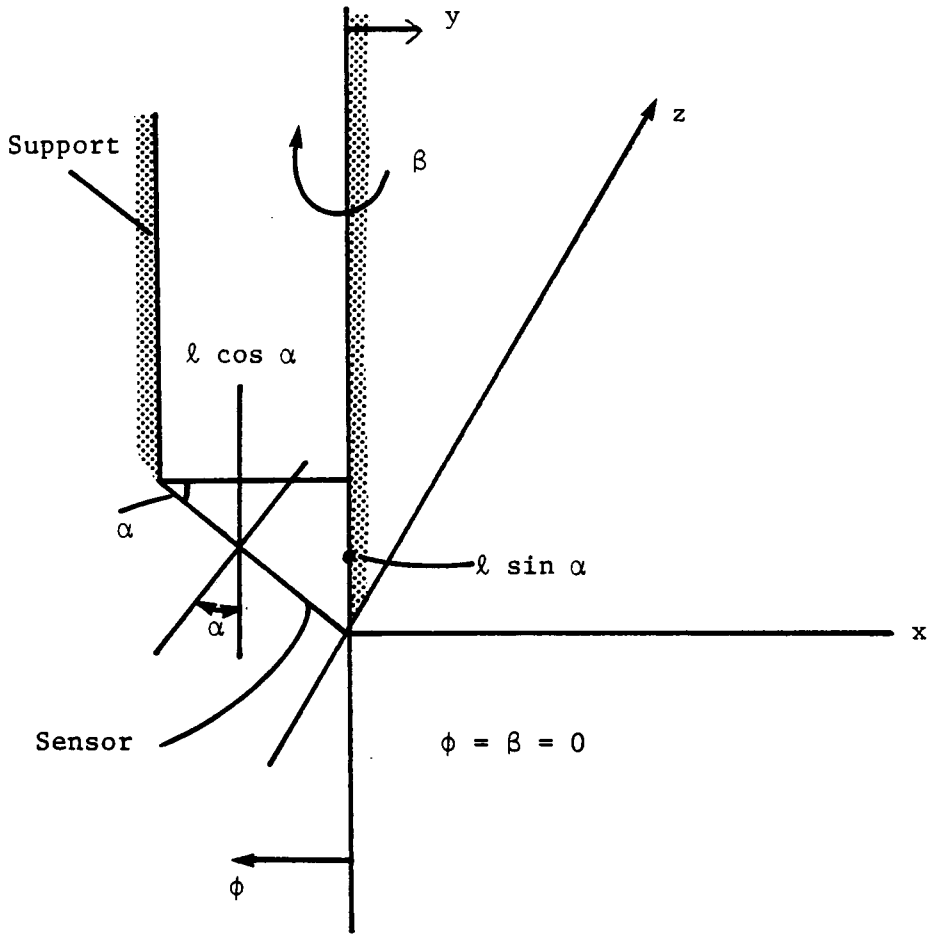

Figure A.2 Slant Probe in Reference Coordinate System

Notice that rotations of ϕ and β are perpendicular and do not affect one another.

Taking the origin at the foot of the longer probe support per Fig. A.3, and writing equations for the x and y coordinates of the short end of the probe, there result

$$x = -\ell \cos\alpha \cos\beta \cos\phi + \ell \sin\alpha \sin\phi \tag{A.1}$$

$$y = +\ell \cos\alpha \cos\beta \sin\phi + \ell \sin\alpha \cos\phi \tag{A.2}$$

Next consider the projection in the y,z plane with $\phi=0$ and $\beta = +\pi/2$ per Fig. A.4.

The $\ell \sin\alpha$ component shown never projects on z for any ϕ or β. The $\ell \cos\alpha$ component projects as $\ell \cos\alpha \sin\beta$. Therefore, an equation may be written as follows for the z coordinate of the end of the sensor at the short support.

$$z = -\ell \cos\alpha \sin\beta \tag{A.3}$$

A.3.2 Determination of Yaw of the Sensor

Now consider Fig. A.5. With the angle ϕ held at zero as in the main windtunnel, the angles β and θ are identically the same, and locate the vertical plane tangent to the local streamline. The angle ω locates the direction of flow in that vertical tangent plane to the streamline. The angle θ is known from nulling the probe. The U_s and U_y velocity components are known from the experimental data inserted into

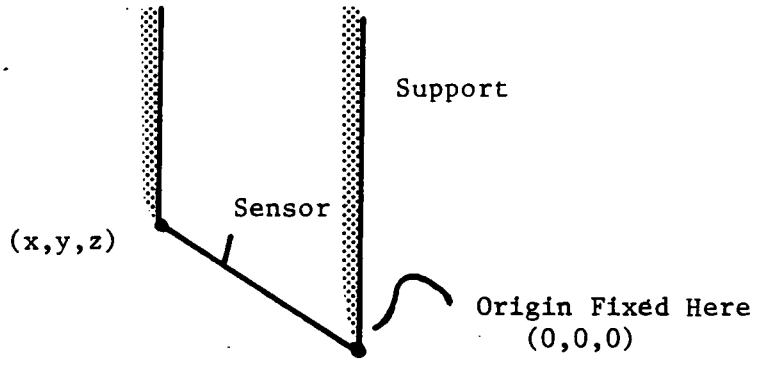

Figure A.3 Location of Origin of Coordinate System

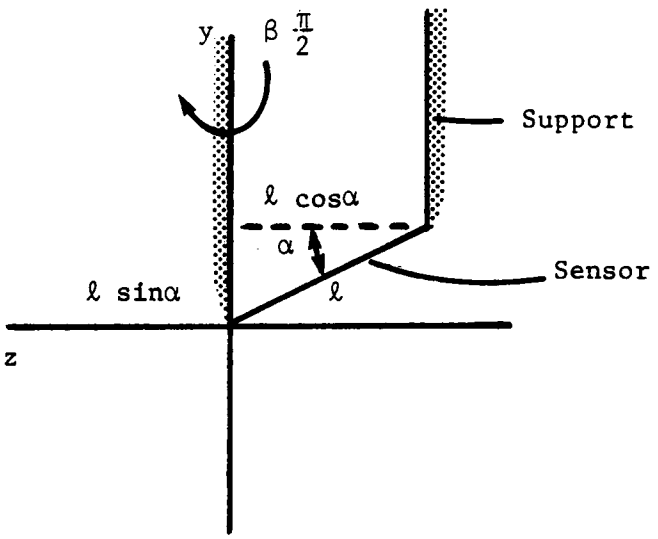

Figure A.4 Projection of Slant Probe in y,z Plane

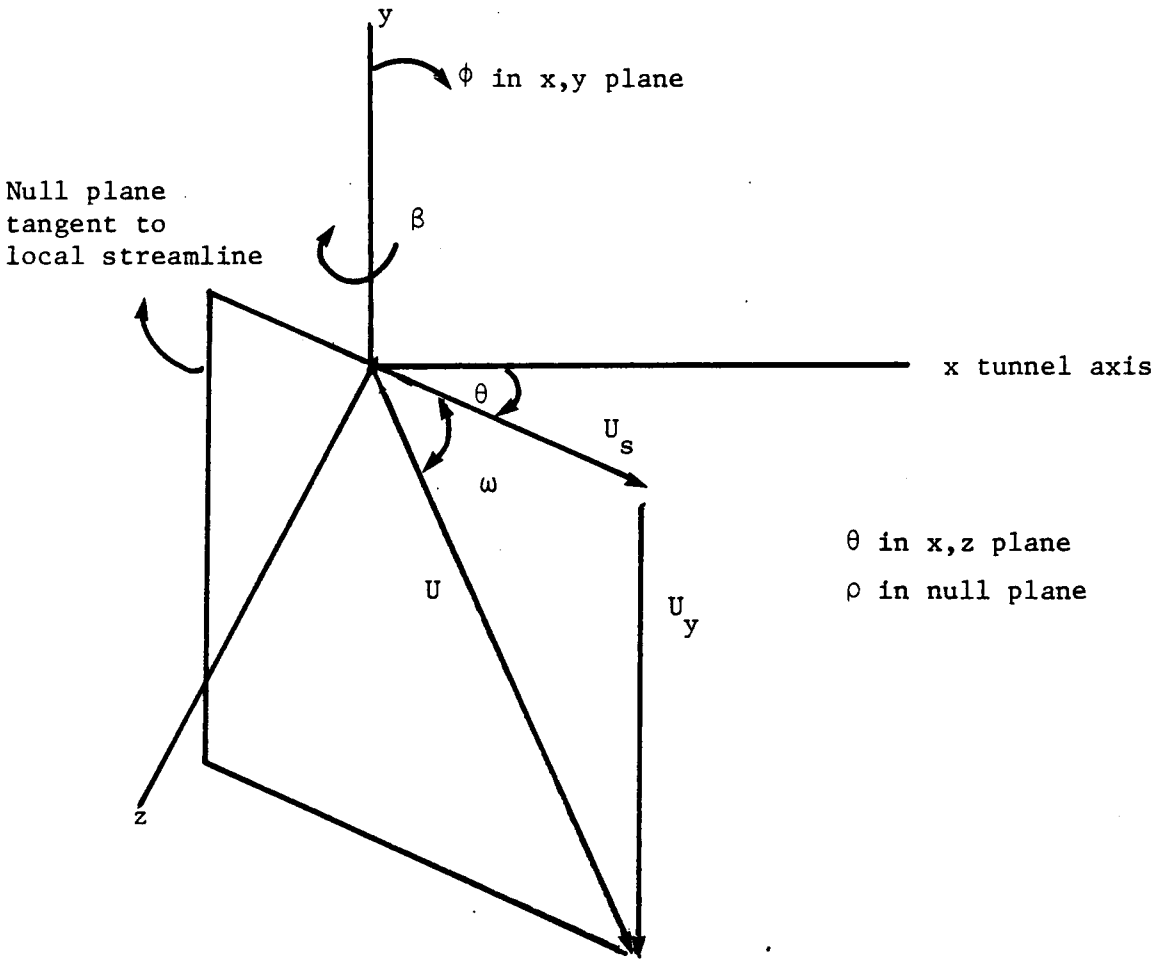

Figure A.5 Vertical Plane of Local Streamline Tangent

the constant k and h MHK expressions, and perhaps subsequently iterated for more accuracy. Immediately there follows

$$\omega = - \arctan \frac{U_y}{U_s} \tag{A.4}$$

U_n equals zero from streamline definition.

An expression can then be written from the diagram for U:

$$U = \sqrt{U_s^2 + U_y^2} \left[\cos \omega \cos \theta \, \bar{i} - \sin \omega \, \bar{j} + \cos \omega \sin \theta \, \bar{k}\right] \tag{A.5}$$

The vector describing the sensor position is

$$\bar{w} = \frac{x}{\ell} \bar{i} + \frac{y}{\ell} \bar{j} + \frac{z}{\ell} \bar{k} \tag{A.6}$$

substituting from Eqs. A.1, A.2, and A.3.

Taking the dot product and normalizing, there results:

$$\cos \delta = \frac{x}{\ell} \cos \omega \cos \theta - \frac{y}{\ell} \sin \omega + \frac{z}{\ell} \cos \omega \sin \theta \tag{A.7}$$

where δ is the desired yaw angle relating the velocity and sensor.

A.3.3 Determination of Pitch of the Sensor

Consider next Fig. A.6, which shows a general illustration of a slant probe in a flow, with velocity decomposed into tangential and supernormal components. The supernormal is further decomposed into normal and binormal components.

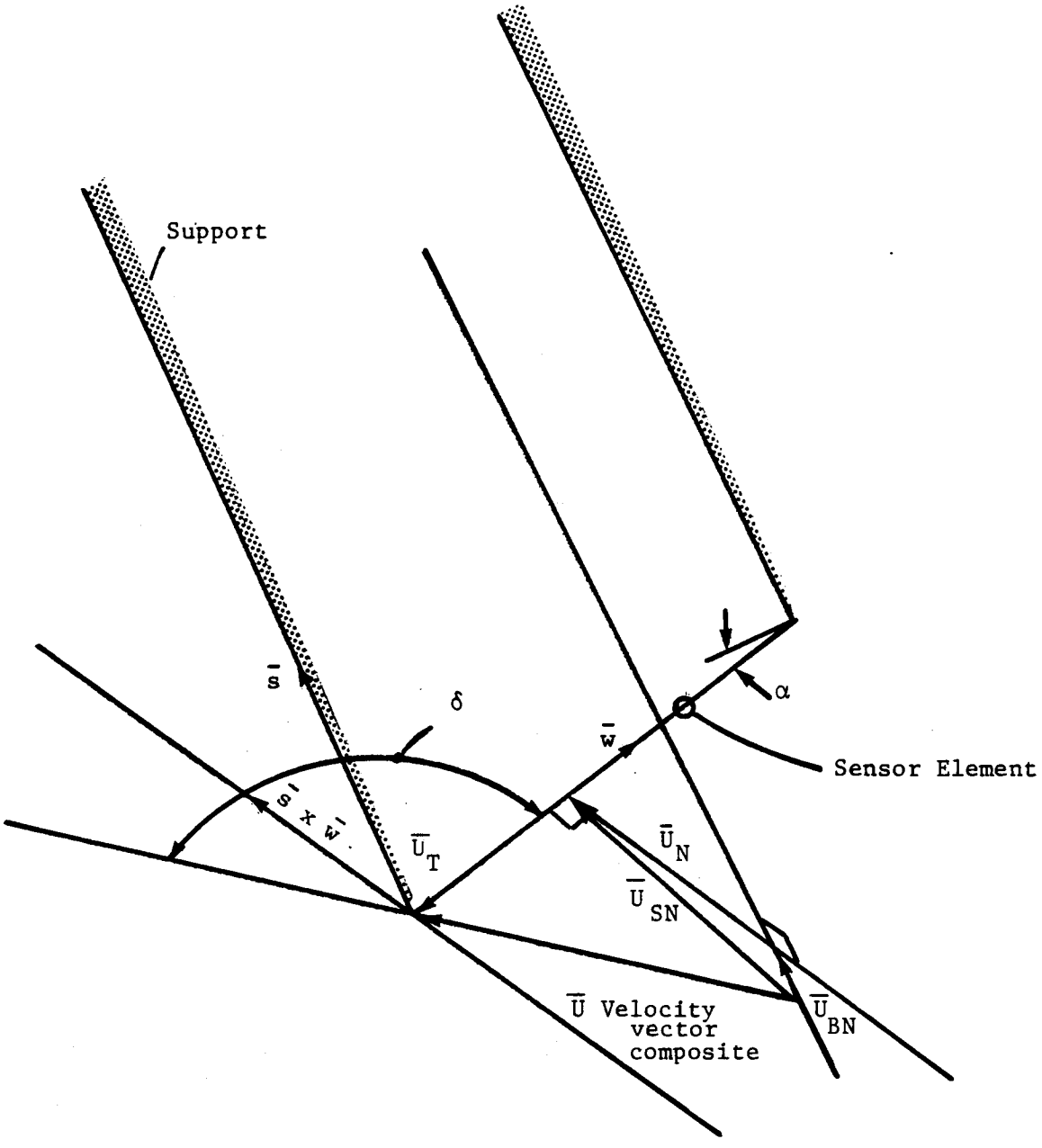

Figure A.6 Velocity Diagram on Slant Sensor in General Flow Field

The vector $\bar{w}$ of the sensor is shown. Also a vector $\bar{s}$ may be defined on and along the longer probe support with its tail at the sensor junction.

$$\bar{s} = \sin\phi\,\bar{i} + \cos\phi\,\bar{j} \tag{A.8}$$

The cross product of $\bar{s}$ and $\bar{w}$ defines the plane of the probe supports

$$\bar{s} \times \bar{w} = +\,z\cos\phi\,\bar{i} - z\sin\phi\,\bar{j} + (y\sin\phi - x\cos\phi)\,\bar{k} \tag{A.9}$$

Also, Fig. A.6 may be used to aid in writing the following expressions for the tangential, supernormal, binormal, and normal velocity components. These are useful in calculating k and h as will be shown later.

$$\bar{U}_T = = U\cos\delta\,\bar{w} \tag{A.10}$$

$$\bar{U}_{SN} = \bar{U} + U\cos\delta\,\bar{w} \tag{A.11}$$

$$\bar{U}_N = \left[\overline{U_{SN}} \cdot (\bar{s} \times \bar{w})_{unit}\right] (\bar{s} \times \bar{w})_{unit} \tag{A.12}$$

$$\bar{U}_{BN} = \bar{U}_{SN} - \bar{U}_N \tag{A.13}$$

The definition for pitch of velocity relative to the sensor is chosen as

$$\bar{U}_{unit} \cdot (\bar{w} \times \bar{s})_{unit} = \cos(P - \tfrac{\pi}{2}) = \sin P \tag{A.14}$$

A.4 Generation of Jorgenson k and h as Functions of Yaw and Pitch

Making use of the foregoing results, in the calibration rig, the velocity vector has a known direction down the tunnel and its magnitude may easily be determined by a Kiel probe and manometer. β and ϕ are manually varied, and anemometer voltage is recorded for reduction to find Jorgenson k and h corresponding to the position.

In this work, k is assumed to be a function of yaw only. Also h is is taken as solely a function of pitch.

A.4.1 Determination of Jorgenson k for a Horizontal Probe

For the horizontal probe note that yaw of the probe support equals yaw of the sensor if $\phi=0$. Under such conditions in the calibration tunnel, the U_{BN} component is zero (see Fig. A.7) and the Jorgenson law reduces to

$$U_{eff}^2 = U_N^2 + k^2 U_T^2 \tag{A.15}$$

U_{eff}^2 comes from E_ℓ^2/S^2. It can be seen from Fig. A.7 that $U_N^2 = U^2\cos^2\beta$ and $U_T^2 = U^2\sin^2\beta$.

Equation A.15 may easily then be solved for k as β is varied over the entire range of 0 through 360°.

A.4.2 Determination of Jorgenson h for a Horizontal Probe

Having k over the entire range of yaw angles, both pitch and yaw of the probe body may be varied to allow a complete range of pitch angles of the sensor.

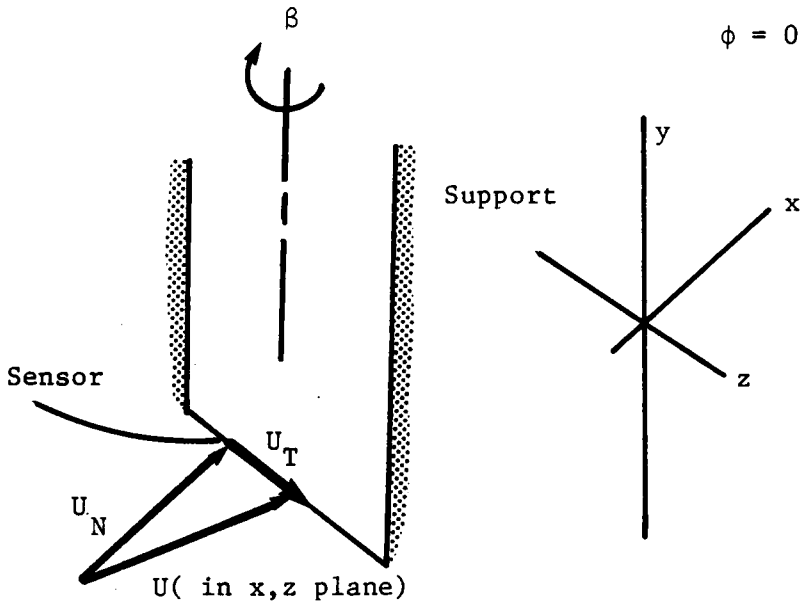

Figure A.7 Horizontal Sensor Undergoing Pure Yaw Deviations

Because the flow direction and velocity are known in the calibration tunnel, the sensor yaw and pitch, and the normal, tangential, and binormal velocity components immediately follow from the analyses of Section A.3. The only unknown in the complete Jorgenson's law expression ($U_{eff}^2 = U_{BN}^2 + k^2U_T^2 + h^2U_N^2$) is h, and it may be readily calculated.

As to the determination of the locus of points at which data is taken, the foregoing analysis has been implemented on the computer to result in a tabulation of yaw and pitch of the sensor in terms of yaw and pitch of the probe over the possible range of probe movements. This is presented in Tables A.1 and A.2. A selection of "best" points can be made for calibration. Assumptions made about symmetry may perhaps be beneficial in covering the entire range of pitch.

A specific possibility, referring to Fig. A.8, is that with β held at $\pi/2$, the pitch of the probe is the pitch of the sensor over the range of the calibration rig, from -25° to 57°. This scheme has the advantages that the tangential component of velocity is always zero, thus eliminating evaluation of k to determine h, and that it covers a large part of the necessary range of pitch.

A.4.3 Determination of Jorgenson k for a Slant Probe

Refer to Fig. A.9. To determine k and h for the slant probe, note that with $\beta = 0°$ or 180° variation of ϕ results in changing the yaw of the sensor element relative to the flow, but not its pitch. In this situation there is never a normal component of velocity, such that the Jorgenson law reduces to

PITCH ANGLE OF PROBE IN DEGREES

YAW ANGLE OF PROBE	55	50	45	40	35	30	25	20	15	10	5	0	-5	-10	-15	-20	-25
0	55	50	45	40	35	30	25	20	15	10	5	0	5	10	15	20	25
10	56	51	46	41	36	31	27	22	18	14	11	10	11	14	18	22	27
20	57	53	48	44	40	36	32	28	25	22	21	20	21	22	25	28	32
30	60	56	52	48	45	41	38	36	33	31	30	30	30	31	33	36	38
40	64	61	57	54	51	48	46	44	42	41	40	40	40	41	42	44	46
50	68	66	63	61	58	56	54	53	52	51	50	50	50	51	52	53	54
60	73	71	69	67	66	64	63	62	61	61	60	60	60	61	61	62	63
70	79	77	76	75	74	73	72	71	71	70	70	70	70	70	71	71	72
80	84	84	83	82	82	81	81	81	80	80	80	80	80	80	80	81	81
90	90	90	90	90	90	90	90	90	90	90	90	90	90	90	90	90	90
100	84	84	83	82	82	81	81	81	80	80	80	80	80	80	80	81	81
110	79	77	76	75	74	73	72	71	71	70	70	70	70	70	71	71	72
120	73	71	69	67	66	64	63	62	61	61	60	60	60	61	61	62	63
130	68	66	63	61	58	56	54	53	52	51	50	50	50	51	52	53	54
140	64	61	57	54	51	48	46	44	42	41	40	40	40	41	42	44	46
150	60	56	52	48	45	41	38	36	33	31	30	30	30	31	33	36	38
160	57	53	48	44	40	36	32	28	25	22	21	20	21	22	25	28	32
170	56	51	46	41	36	31	27	22	18	14	11	10	11	14	18	22	27
180	55	50	45	40	35	30	25	20	15	10	5	0	5	10	15	20	25

TABLE A.1
YAW OF HORIZONTAL SENSOR
VERSUS YAW AND PITCH OF PROBE
SENSOR ANGLES HAVE BEEN CONVERTED
TO HAVE RANGE 0-90 DEGREES

PITCH ANGLE OF PROBE IN DEGREES

YAW ANGLE OF PROBE IN DEGREES	55	50	45	40	35	30	25	20	15	10	5	0	-5	-10	-15	-20	-25
0	90	90	90	90	90	90	90	90	90	90	90	90	90	90	90	90	90
10	83	82	80	78	76	73	70	64	57	45	27	0	27	45	57	64	70
20	77	74	71	68	64	59	54	47	38	27	14	0	14	27	38	47	54
30	71	67	63	59	54	49	43	36	28	19	10	0	10	19	28	36	43
40	66	62	57	53	47	42	36	30	23	15	8	0	8	15	23	30	36
50	62	57	53	48	42	37	31	25	19	13	7	0	7	13	19	25	31
60	59	54	49	44	39	34	28	23	17	12	6	0	6	12	17	23	28
70	57	52	47	42	37	32	26	21	16	11	5	0	5	11	16	21	26
80	55	50	45	40	35	30	25	20	15	10	5	0	5	10	15	20	25
90	55	50	45	40	35	30	25	20	15	10	5	0	5	10	15	20	25
100	55	50	45	40	35	30	25	20	15	10	5	0	5	10	15	20	25
110	57	52	47	42	37	32	26	21	16	11	5	0	5	11	16	21	26
120	59	54	49	44	39	34	28	23	17	12	6	0	6	12	17	23	28
130	62	57	53	48	42	37	31	25	19	13	7	0	7	13	19	25	31
140	66	62	57	53	47	42	36	30	23	15	8	0	8	15	23	30	36
150	71	67	63	59	54	49	43	36	28	19	10	0	10	19	28	36	43
160	77	74	71	68	64	59	54	47	38	27	14	0	14	27	38	47	54
170	83	82	80	78	76	73	70	64	57	45	27	0	27	45	57	64	70
180	90	90	90	90	90	90	90	90	90	90	90	180	90	90	90	90	90

TABLE A.2
PITCH OF HORIZONTAL SENSOR
VERSUS YAW AND PITCH OF PROBE
SENSOR ANGLES HAVE BEEN CONVERTED
TO HAVE RANGE 0-90 DEGREES

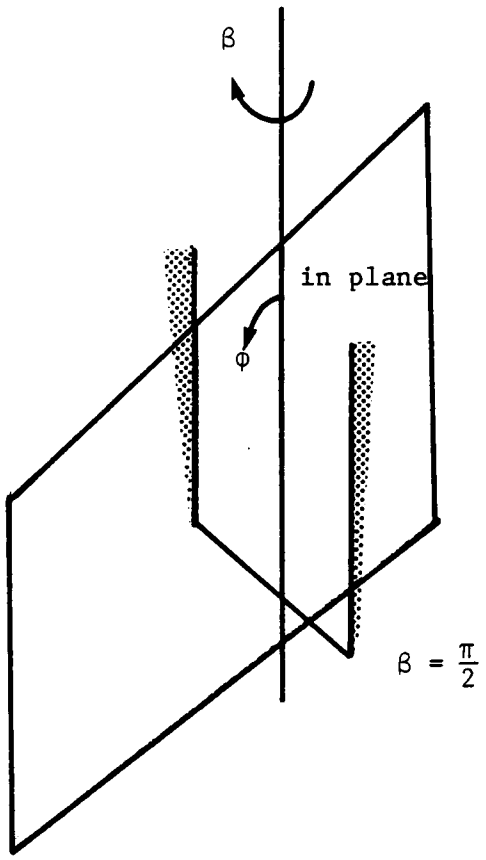

Figure A.8 Horizontal Sensor Undergoing Pure Pitch Deviations

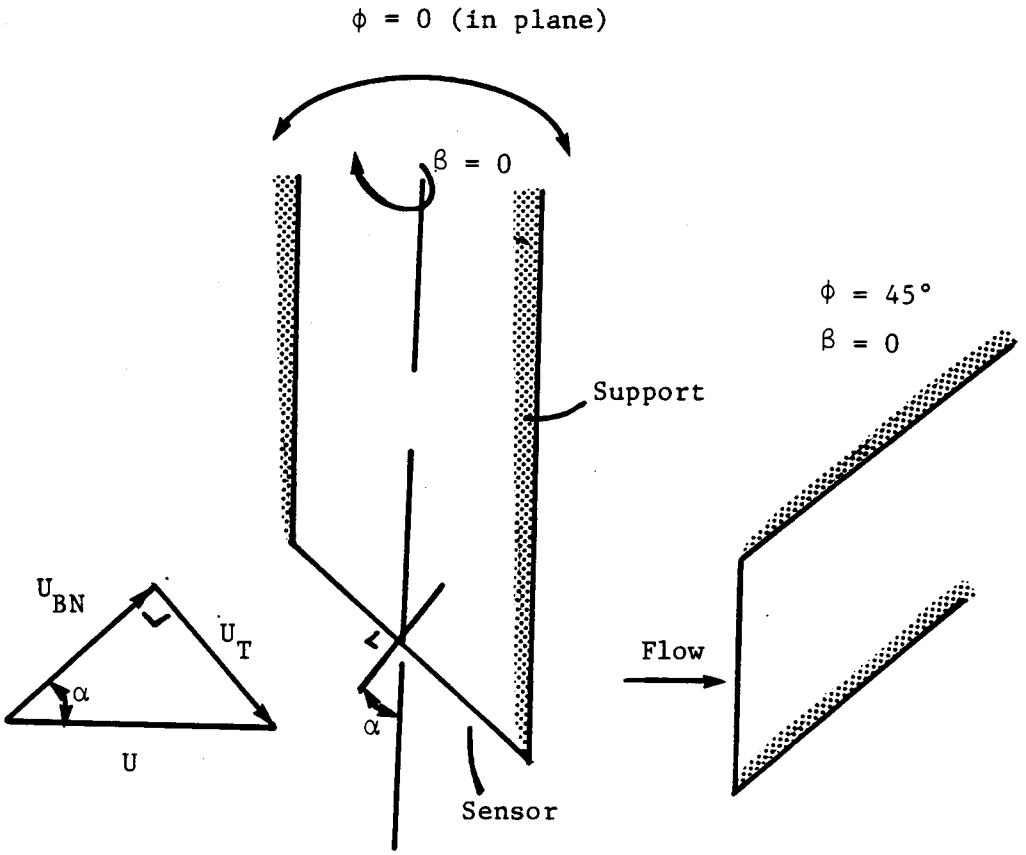

$U_N \perp$ page

$U_N = 0$ for $\psi = 0, 180°$

Figure A.9 Slant Sensor Undergoing Pure Yaw Deviations

$$U_{eff}^2 = U_{BN}^2 + k^2 U_T^2 \tag{A.16}$$

Again

$$U_{eff}^2 = E_\ell^2/S^2$$

Also from Fig. 3.5 it is evident that

$$U_{BN}^2 = U^2 \cos^2(\phi - 45°)$$

$$U_T^2 = U^2 \sin^2(\phi - 45°)$$

and the yaw coefficient, k, may be readily determined.

Some assumptions about symmetry of the probe characteristic must be made to cover the full range of yaw angles.

A.4.4 Determination of Jorgenson h for a Slant Probe

This procedure parallels that of Section A.4.2.2 for the horizontal probe except that no suggestions are offered for the locus of data points. Reliance should be made on the tabulation presented in Tables A.3 and A.4 of yaw and pitch of the sensor versus yaw and pitch of the probe over the allowable range of movement. The "best" locus of points may then be selected. Again symmetry may need to be invoked.

PITCH ANGLE OF PROBE IN DEGREES

YAW ANGLE OF PROBE IN DEGREES	55	50	45	40	35	30	25	20	15	10	5	0	-5	-10	-15	-20	-25
0	80	85	90	85	80	75	70	65	60	55	50	45	40	35	30	25	20
10	80	85	90	85	81	76	71	66	61	56	51	46	41	36	31	26	22
20	79	83	88	87	82	77	72	68	63	58	53	48	44	39	34	30	26
30	77	81	86	89	84	80	75	71	66	61	57	52	48	43	39	35	31
40	74	79	83	88	88	83	79	75	70	66	61	57	53	49	45	41	38
50	71	76	80	84	88	88	84	79	75	71	67	63	59	55	52	48	45
60	68	72	76	79	83	87	89	85	81	77	73	69	66	62	58	55	52
70	64	67	71	74	78	82	85	89	87	83	80	76	72	69	65	62	59
80	59	62	66	69	72	76	79	83	86	90	87	83	79	76	72	69	66
90	55	57	60	63	66	69	73	76	79	83	86	90	86	83	79	76	73
100	49	52	54	57	60	63	66	69	72	76	79	83	87	90	86	83	79
110	44	46	48	50	53	56	59	62	65	69	72	76	80	83	87	89	85
120	39	40	41	44	46	49	52	55	58	62	66	69	73	77	81	85	89
130	33	34	35	37	39	42	45	48	52	55	59	63	67	71	75	79	84
140	27	27	28	30	32	35	38	41	45	49	53	57	61	66	70	75	79
150	21	21	21	23	25	28	31	35	39	43	48	52	57	61	66	71	75
160	16	14	14	16	18	22	26	30	34	39	44	48	53	58	63	68	72
170	12	8	7	9	13	17	22	26	31	36	41	46	51	56	61	66	71
180	10	5	0	5	10	15	20	25	30	35	40	45	50	55	60	65	70

TABLE A.3
YAW OF SLANT SENSOR
VERSUS YAW AND PITCH OF PROBE
SENSOR ANGLES HAVE BEEN CONVERTED
TO HAVE RANGE 0-90 DEGREES

PITCH ANGLE OF PROBE IN DEGREES

YAW ANGLE OF PROBE IN DEGREES	55	50	45	40	35	30	25	20	15	10	5	0	-5	-10	-15	-20	-25
0	90	90	90	90	90	90	90	90	90	90	90	90	90	90	90	90	90
10	84	84	83	82	82	81	80	80	79	78	77	76	75	73	71	68	65
20	78	77	76	75	74	72	71	70	68	67	65	63	60	58	54	50	44
30	73	71	69	67	66	64	62	60	58	56	53	51	48	44	40	35	29
40	67	65	63	60	58	56	54	51	49	46	43	40	37	33	29	24	18
50	62	59	57	54	51	48	46	43	40	37	34	31	27	23	19	14	9
60	58	54	51	48	44	41	38	35	32	29	26	22	19	15	11	6	2
70	53	49	45	42	38	35	31	28	25	21	18	14	11	7	3	1	5
80	49	44	40	36	32	28	25	21	18	14	11	7	4	0	4	8	12
90	45	40	35	31	26	22	18	14	11	7	4	0	4	7	11	14	18
100	42	36	31	26	21	16	12	8	4	0	4	7	11	14	18	21	25
110	39	33	26	21	15	10	5	1	3	7	11	14	18	21	25	28	31
120	37	29	22	15	9	4	2	6	11	15	19	22	26	29	32	35	38
130	36	27	18	10	3	3	9	14	19	23	27	31	34	37	40	43	46
140	36	25	14	5	4	12	18	24	29	33	37	40	43	46	49	51	54
150	38	25	11	2	13	22	29	35	40	44	48	51	53	56	58	60	62
160	45	28	7	12	26	37	44	50	54	58	60	63	65	67	68	70	71
170	61	40	4	31	49	59	65	68	71	73	75	76	77	78	79	80	80
180	90	90	180	90	90	90	90	90	90	90	90	90	90	90	90	90	90

TABLE A.4
PITCH OF SLANT SENSOR
VERSUS YAW AND PITCH OF PROBE
SENSOR ANGLES HAVE BEEN CONVERTED
TO HAVE RANGE 0-90 DEGREES

A.4.5 Relation of the Foregoing Analysis to the Installation of the Probe in the Main Tunnel

Refer to Fig. 2.1 presented earlier for coordinate definition. Relating this analysis to the main tunnel, the angle α of the sensor is known. The angle ϕ always equals zero. Angle θ is found from nulling. Angle β, which represents here deviation of the support plane from the tunnel axis, is replaced by $\phi+\theta$ in Fig. 2.1. Equation A.6 may be used to define sensor position. Equation A.5 is used for the velocity vector. From Eq. A.8 comes the yaw angle of the probe sensor relative to local velocity. $(\overline{s} \times \overline{w})$ follows from Eq. A.9 with $\phi=0$. Equations A.11 and A.14 are then used for pitch of the sensor.

APPENDIX B

LISTING OF THE MHK EQUATION REDUCTION CODE

```
C
C
C
C
C
C
C
C                    APPENDIX B
C
C
C        LISTING OF MHK EQUATION REDUCTION CODE
C
C
C
C
C                  VARIABLE LISTING
C
C
C
C      A1      NON DIMENSIONALIZED TURBULENT QUANTITY
C      A2      NON DIMENSIONALIZED TURBULENT QUANTITY
C      A3      NON DIMENSIONALIZED TURBULENT QUANTITY
C      A4      NON DIMENSIONALIZED TURBULENT QUANTITY
C      AH      HORIZONTAL PROBE NULL ANGLE
C      ALF     SENSOR-SUPPORT ANGLE
C      AS      SLANT PROBE NULL ANGLE
C      BH      CALIBRATION CURVE INTERCEPT HORIZONTAL PROBE
C      BS      CALIBRATION CURVE INTERCEPT SLANT PROBE
C      HH      JORGENSON H SQUARED , HORIZONTAL PROBE
C      HS      JORGENSON H SQUARED , SLANT PROBE
C      Q1      RMS VOLTS HORIZONTAL PROBE  90 DEG
C      Q2      RMS VOLTS SLANT PROBE   0 DEG
C      Q3      RMS VOLTS SLANT PROBE   180 DEG
C      Q4      MEAN VOLTS  SLANT PROBE   180 DEG
C      Q5      MEAN VOLTS SLANT PROBE    0 DEG
C      Q6      RMS VOLTS HORIZONTAL PROBE  -45 DEG
C      Q7      RMS VOLTS HORIZONTAL PROBE   45 DEG
C      Q8      MEAN VOLTS HORIZONTAL PROBE 90 DEG
C      Q9      RMS VOLTS   SLANT PROBE    25 DEG
C      Q10     RMS VOLTS SLANT PROBE      -25 DEG
C      SH      LINEARIZER SLOPE  HORIZONTAL PROBE
C      SS      LINEARIZER SLOPE SLANT PROBE
C      SY      ANGLE 25 DEG
C      T(**)   TURBULENT STRESSES
```

```
C       TH      NULL ANGLE
C       U       VELOCITY
C       US      STREAMLINE VELOCITY
C       UTAU    SHEAR VELOCITY
C       UX      X VELOCITY
C       UY      Y VELOCITY


C       UZ      Z VELOCITY
C       Y       ELEVATION
C       YH      ELEVATION HORIZONTAL PROBE
C       YS      ELEVATION SLANT PROBE
C       YT      INTERMEDIATE TENSOR
C       Z       DUMMY VARIABLE
C       ZKH     JORGENSON K SQUARED , HORIZONTAL PROBE
C       ZKS     JORGENSON K SQUARED , SLANT PROBE
C       ZL(**)  DIRECTION COSINE MATRIX
C       ZT      INTERMEDIATE TENSOR
C
C
C
C
C
C
C
C  THIS PROGRAM READS ANEMOMETER OUTPUT VOLTAGE DATA FROM FILES
C  TRANSMITTED BY TELEPHONE BY THE TRS-80 RADIO SHACK COMPUTER
C  IN THE DIGITAL ACQUISITION SYSTEM. IT THEN CALCULATES MEAN VELOCITIES
C  AND TURBULENT STRESSES FROM THE ANALYSIS BY MHK OF GA TECH.
C  COORDINATE TRANSFORMATIONS ARE THEN PERFORMED FROM SYN TO XYZ.
C$JOB
      DIMENSION T(3,3)
C  INPUT CALIBRATION AND FLOW PARAMETERS. INCLUDE CALCULATED UTAU
C  VALUE FOR NON-DIMENSIONALIZING,THEN ANGLE OF SLANT PROBE,
C  THEN SLOPE & INTERCEPT OF CALIBRATION CURVE, AND JORGENSON H**2
C  & K**2 VALUES, FIRST FOR HORIZONTAL, THEN SLANT PROBES.
C       SHEAR VELOCITY AND SLANT PROBE SENSOR-SUPPORT ANGLE FOLLOW
      UTAU=2.85
      ALF=.7854
C       HORIZONTAL PROBE LINEARIZER SLOPE,INTERCEPT,AND
C       JORGENSON K AND H SQUARED FOLLOW
      SH=.03117319
```

```
      BH=.000
      ZKH=.09328
      HH=1.0
C       SLANT PROBE LINEARIZER SLOPE,INTERCEPT, AND
C       JORGENSON K AND H SQUARED FOLLOW
      SS= .03415773
      BS= .000
      ZKS=.26498
      HS=1.0
      PRINT 90
   90 FORMAT(1X,47HTHE FOLLOWING WERE CALCULATED FROM MHK          )
   91 FORMAT(10X,12HFILE IDS     )
      PRINT 94
      PRINT 94
C READ VOLTAGES AT THE VARIOUS ANGULAR POSITIONS OF THE SENSORS.
C FILE 30 IS FOR HORIZONTAL ,20 FOR SLANT.
      READ(30,95)
      READ(20,88)
   95 FORMAT(  ////////////)
   88 FORMAT( /////////////)
   82 READ(30,*)YH.AH


      READ(20,*)YS,AS
      READ(30,94)
      READ(20,94)
   94 FORMAT(/ )
      READ(20,*)Q4,Z,Q3,Z,Z,Z,Q9,Z,Q5,Z,Q2,Z,Z,Z,Q10,Z
      READ(30,*)Q8,Z,Q1,Z,Z,Z,Q7,Z,Z,Z,Q6,Z
C     PRINT 81,Q1,Q2,Q3,Q4,Q5
C     PRINT 81,Q6,Q7,Q8,Q9,Q10
C SQUARE THE RMS FLUCTUATING VOLTAGE COMPONENTS, AND CORRECT MEAN
C VOLTAGES FOR CALIBRATION CURVE INTERCEPT.
      Q1=Q1**2
      Q2=Q2**2
      Q3=Q3**2
      Q4=Q4-BS
      Q5=Q5-BS
      Q6=Q6**2
      Q7=Q7**2
      Q8=Q8-BH
      Q9=Q9**2
```

```
      Q10=Q10**2
C SOLVE THE GT EQUATIONS SUCCESSIVELY
C INDEX 1 STANDS FOR S DIRECTION
C INDEX 2 STANDS FOR Y DIRECTION
C INDEX 3 STANDS FOR N DIRECTION
C THE TWO INDICES DENOTE THE TURBULENT STRESS TENSOR QUANTITY
C     FOR EXAMPLE, T(1,1) CORRESPONDS TO (U(S)U(S)) QTY
      T(1,1)=Q1/SH**2/HH
      T(2,2)=((Q2+Q3)/SS**2/2.0/(SIN(ALF)**2+ZKS*COS(ALF)**2)-
     1T(1,1))*((SIN(ALF)**2+ZKS*COS(ALF)**2)**2)/(1.0-ZKS)**2/
     1SIN(ALF)**2/COS(ALF)**2
      T(1,2)=(Q2-Q3)/SS**2/4.0/(1.0-ZKS)/SIN(ALF)/COS(ALF)
      UY=(Q4-Q5)/SS/2.0*SQRT(SIN(ALF)**2+ZKS*COS(ALF)**2)/
     1(ZKS-1.0)/SIN(ALF)/COS(ALF)
      T(3,3)=(((Q6+Q7)/SH**2/(ZKH+HH))-T(1,1))*(HH+ZKH)**2/
     1(HH-ZKH)**2
      T(1,3)=(Q6-Q7)/SH**2/2.0/(ZKH-HH)
      US=(SQRT(ABS(Q8**2/SH**2-2.0*(UY**2+T(2,2)+ZKH*T(3,3))))+
     1Q8/SH)/2.0/HH
      SY=25.*.017453
      T(2,3)=((Q10-Q9)/SS**2/4.0/COS(SY)/SIN(SY)/(SIN(ALF)**2+
     1ZKS*COS(ALF)**2-HS)-T(1,3))*(COS(SY)**2*SIN(ALF)**2
     1+ZKS*COS(SY)**2*COS(ALF)**2+HS*SIN(SY)**2)/
     1(1.0-ZKS)/COS(SY)/SIN(ALF)/COS(ALF)
C DETERMINE STRESSES ACROSS THE MAIN DIAGONAL
      T(2,1)=T(1,2)
      T(3,1)=T(1,3)
      T(3,2)=T(2,3)
      Y=(YH+YS)/2.
      TH=-(AH+AS)/2.*.017453
C DO COORDINATE TRANSFORMATION BY SUCCESSIVE TENSOR MULTIPLICATIONS
C IN SUBROUTINE COORDS. ALSO XFORM MEAN VELOCITIES.
      CALL COORDS(U,US,UY,UN,T,GZT,TH,UX,UZ)
      PRINT 64
   64 FORMAT (20X,18HTURBULENT STRESSES)
      PRINT 97


C PRINT TENSOR QUANTITIES
   97 FORMAT(1X,9HELEVATION,4X,2HUU,7X,2HVV,7X,2HWW,7X,2HUV,
     X7X,2HUW,7X,2HVW)
      PRINT 96,Y,T(1,1),T(2,2),T(3,3),T(1,2),T(1,3),T(2,3)
```

```
   96 FORMAT(2X,8F9.4)
C   NON-DIMENSIONALIZE TURBULENT VELOCITY COMPONENTS BY UTAU & PRINT
      A1=SQRT(ABS(T(1,1)))/UTAU
      A2=SQRT(ABS(T(2,2)))/UTAU
      A3=SQRT(ABS(T(3,3)))/UTAU
      A4=ABS(T(1,2))/UTAU**2
      PRINT 65
   65 FORMAT (20X,27HNONDIMENSIONALIZED STRESSES)
      PRINT 98
   98 FORMAT(10X,2X,7HU'/UTAU,2X,7HV'/UTAU,2X,7HW'/UTAU,
     X2X,11H-UV/UTAU**2)
      PRINT 62,A1,A2,A3,A4
   62 FORMAT(11X,7F9.4)
      WRITE(40,62)Y,A1,A2,A3,A4
C PRINT MEAN VELOCITIES
      PRINT 66
   66 FORMAT (20X,15HMEAN VELOCITIES)
      PRINT 99
   99 FORMAT(14X,1HU,8X,2HUS,7X,2HUY,7X,2HUX,7X,2HUZ)
      PRINT 62,U,US,UY,UX,UZ
      PRINT 94
      WRITE(45,62) Y,US
C REPEAT FOR NEXT ELEVATION
      GO TO 82
   81 FORMAT (2X,6E13.4)
  166 FORMAT(2X,3E13.4)
  113 FORMAT (2X,8E13.4)
      STOP
      END
      SUBROUTINE COORDS (U,US,UY,UN,T,ZT,TH,UX,UZ)
C  SUBROUTINE FOR COORDINATE TRANSFORM
      DIMENSION ZL(3,3),T(3,3),YT(3,3),ZT(3,3)
      UN=0.0
C SET DIRECTION COSINES
      ZL(1,1)=COS(TH)
      ZL(1,2)=0.0
      ZL(1,3)=-SIN(TH)
      ZL(2,1)=0.0
      ZL(2,2)=1.0
      ZL(2,3)=0.0
      ZL(3,1)=-SIN(TH)
      ZL(3,2)=0.0
      ZL(3,3)=COS(TH)
C PERFORM MATRIX MULTIPLICATION FOR STRESS XFMN (2 CYCLES)
```

```
      DO 1 I=1,3
      DO 2 L=1,3
      YT(I,L)=0.0
      DO 3 J=1,3
      YT(I,L)=ZL(J,L)*T(I,J)+YT(I,L)
    3 CONTINUE
    2 CONTINUF


    1 CONTINUE
      DO 4 M=1,3
      DO 5 L=1,3
      ZT(M,L)=0.0
      DO 6 I=1,3
      ZT(M,L)=ZL(I,M)*YT(I,L)+ZT(M,L)
    6 CONTINUE
    5 CONTINUE
    4 CONTINUE
C TRANSFORM LINEAR VELOCITIES
      UX=US*COS(TH)-UN*SIN(TH)
      UZ=US*SIN(TH)+UN*COS(TH)
      U=SQRT(UX**2+UY**2+UZ**2)
      RETURN
      END
C$ENTRY
```

The vita has been removed from the scanned document